Arabian Journal of Chemistry (2023) **16**, 104502

King Saud University

Arabian Journal of Chemistry

www.ksu.edu.sa
www.sciencedirect.com

REVIEW ARTICLE

SAR studies of quinoline and derivatives as potential treatments for Alzheimer's disease

Zhao-Hui Li [a,1], Li-Quan Yin [b,1], Dong-Hai Zhao [c], Lian-Hai Jin [c], Ya-Juan Sun [d,*], Cheng Tan [e,*]

[a] *Department of Neurosurgery, China-Japan Union Hospital of Jilin University, Changchun 130033, Jilin, PR China*
[b] *Department of Rehabilitation Medicine, China-Japan Union Hospital of Jilin University, Changchun 130033, PR China*
[c] *Jilin Medical University, Jilin, Jilin Province 132013, PR China*
[d] *Department of Neurology, China-Japan Union Hospital of Jilin University, Changchun 130033, Jilin, PR China*
[e] *Department of Emergency, China-Japan Union Hospital of Jilin University, Changchun 130033, PR China*

Received 27 September 2022; accepted 4 December 2022
Available online 9 December 2022

KEYWORDS

Quinoline;
Anti-Alzheimer;
Multitarget-directed ligand;
Acetylcholinesterase;
Structure–activity relationship;
Neuroprotective activity

Abstract Quinoline analogs are an important class of *N*-based heterocyclic compounds, which have received extensive attention because of their use in medicinal chemistry and organic synthesis. Over the past few decades, several new scaffold-based functionalization synthesis strategies have been reported for quinolines. Quinoline derivatives have a wide range of biological activities, including anti-Alzheimer's disease activity. Herein, we review research on quinoline and related analogs as anti-Alzheimer's disease agents from 2001 to 2022 and particularly highlight the structure–activity relationships and molecular binding modes. This review provides information for the rational design of more effective and target-specific drugs for Alzheimer's disease.

1. Introduction

Alzheimer's disease (AD) is a highly complex neurodegenerative disease, which mainly affects people over the age of sixty, and much research has been devoted to the occurrence and development of its pathology (Iqbal and Grundke-Iqbal, 2000, De-Paula, et al., 2012, Anand, et al., 2014, Kim, et al., 2021, Long and Holtzman, 2019, Gerring, et al., 2021). >46 million people worldwide are estimated to be affected by AD, and by 2050, 131.5 million people will suffer from this neurodegenerative disease (Prince, et al., 2015, Lemes, et al., 2016, Obulesu and Jhansilakshmi, 2014, Lee, et al., 2020, Kim, et al., 2020, Pan, et al., 2020). The pathogenesis of AD is not fully understood; however, many factors, including beta-amyloid (Aβ) deposition, oxidative stress, tau protein aggregation, reduced acetylcholine (ACh) levels, neuro-inflammation, and bimetallic imbalance,

Abbreviations: AD, Alzheimer's disease; Aβ, beta-amyloid; ACh, acetylcholine; SAR, structure–activity relationship; AChE, acetylcholinesterase; BuChE, butyrylcholinesterase; PAS, peripheral anionic site; PD, Parkinson's Disease; MAO, monoamine oxidase; APP, precursor protein; *h*ChE, human cholinesterase; *h*AChE, human acetylcholinesterase; *h*BChE, human butyrylcholinesterase; *ee*AChE, esterase acetylcholinesterase

* Corresponding authors.
E-mail addresses: SunYaj@jlu.edu.cn (Y.-J. Sun), tancheng@jlu.edu.cn (C. Tan).

[1] These authors contributed equally to this work.

Peer review under responsibility of King Saud University.

Production and hosting by Elsevier

https://doi.org/10.1016/j.arabjc.2022.104502

are believed to be involved in the pathogenesis of AD (Jakob-Roetne and Jacobsen, 2009, Shaik, et al., 2016, Sharma and Kumar, 2009, Bondi, et al., 2017, Hampel et al., 2018, Solis et al., 2020).

Quinoline (also known as 1-azanaphthalene and benzopyridine) is a heterocyclic aromatic organic compound (Nainwal, et al., 2019, Kaur and Kumar, 2021, Corio, et al., 2021, Patil, et al., 2021, Di Mola, et al., 2019, Marasco, et al., 2021, Kankanala, et al., 2016). Coal tar remains the main commercial source, although many reactions have been developed to synthesize quinoline. Quinoline and quinoline derivatives exist widely in nature (Baccile, et al., 2016, Rivo, et al., 2020, Petruczynik, et al., 2019, Felicetti, et al., 2020, Fabiano-Tixier, et al., 2011, Rao, et al., 2009, Nugraha et al., 2020). Because the quinoline moiety provides an easy-to-use scaffold for the design and synthesis of drugs, quinoline is recognized as a classic privileged structure. The quinoline pharmacophore is an important functionality, which has the potential for a wide range of biological and pharmacological activities, including anti-Alzheimer activity (Chu, et al., 2019, Musiol, 2017, Nqoro, et al., 2017, Rüb, et al., 2017, Shen, et al., 2016, Rani, et al., 2016, Boyd, et al., 2007, Cherny, et al., 2001)(Fig. 1).

Over the past several decades, many quinolone analogs have been designed, synthesized, and screened for pharmacological effects and adverse reactions *in vitro* and *in vivo*, and some compounds possessed considerable activity. This review highlights the recent progress in quinoline derivatives as potential anti-Alzheimer agents. The structure–activity relationship (SAR) and molecular docking studies were reviewed to provide information toward the further design of useful quinoline derivatives.

2. Anti-Alzheimer activity of quinoline and their analogs

Quinoline scaffolds are present in many natural and synthetic compounds with pharmacological activity. Recent studies have demonstrated that some quinoline and quinoline derivatives also have potent anti-acetylcholinesterase (AChE) and anti-butyrylcholinesterase (BuChE) effects. Molecular docking studies have indicated that the quinoline moiety can bind to the peripheral anionic site (PAS) of AChE via π-π stacking interactions (Sang, et al., 2017, Farina, et al., 2015, Shang, et al., 2018). To design drugs for AD, Okamura et al. (Okamura, et al., 2005) have synthesized a quinolone moiety with a phenyl ring substituted at the 2-position (compounds **1** and **2**), which showed higher binding affinity to tau fibrils and lower binding affinity to Aβ fibrils (Fig. 2). The brain uptake after intravenous injection of [^{11}C] **1** was 11.3 %, 5.0 %, 3.1 %, and 2.1 % ID/g at 2, 10, 30, and 60 min, respectively, suggesting that the quinolone moiety is potentially useful in anti-Alzheimer agents.

In AD pathology, iron promotes the accumulation of Aβ peptides and increases the toxicity of Aβ peptides, and iron chelation has been shown to be a feasible neuroprotective strategy. Increased levels of iron in the process of aging and AD will lead to iron-dependent oxidative stress neurodegeneration (Youdim, et al., 2004a). Clioquinol (**3**) promotes metal uptake to target Aβ-responsive synaptic Zn and Cu. Clioquinol (**3**) and the 8-hydroxyquinoline analog (**4**) are shown in Fig. 3a, The Adlard group (Adlard, et al., 2008) has also found that **3** caused metal-induced Aβ-aggregation as an Zn/Cu ionophore and displayed greater blood–brain barrier permeability, which indicated it had potential as a disease-modifying drug for AD. Shachar et al. (Shachar, et al., 2004) have found that **4** could inhibit Fe/ascorbate- and substrate-induced mitochondrial membrane lipid peroxidation (IC_{50} = 12.7 μM) and **4** (1 μg) could also prevent 6-hydroxydopamine-induced striatal dopaminergic damage. In addition, this study showed that **4** exerted neuroprotective effects by acting as a brain-penetrating iron chelator (Fig. 3a). Youdim et al. (Youdim, et al., 2004a) and (Ryan, et al. 2015) have also reported that compounds **4** and **5** displayed activity against the neurodegenerative diseases Parkinson's Disease (PD) and AD (Fig. 3a). In addition, Youdim et al. (Youdim et al., 2005b; Youdim et al., 2006c) have reported that compound **6** was a brain permeable, iron chelating, brain-selective monoamine oxidase (MAO) inhibitor, with a propargyl alcohol neuroprotective effect. Compound **6**

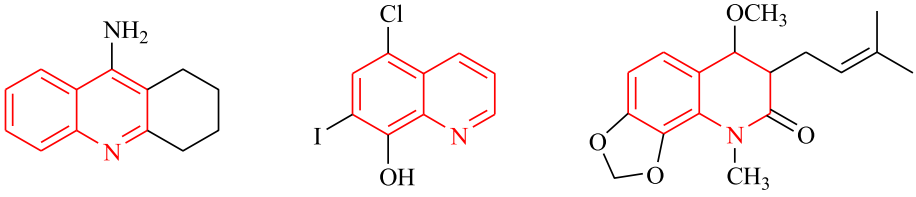

Tacrine Clioquinol Pteleprenine

Fig. 1 There approved anti-Alzheimer containing quinoline moiety.

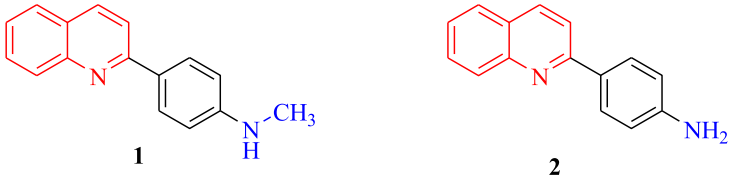

1 **2**

O/W partition coefficient	47.4	70.3
brain uptakes (%ID/g)	11.3(2 min) 3.1(30min)	9.1(2 mi n) 0.25(min)
Ki values for Aβ fibrils (nM)	659	786
EC_{50} for tau fibris (nM)	399	221

Fig. 2 Structural and anti-Alzheimer of quinoline compounds **1,2**.

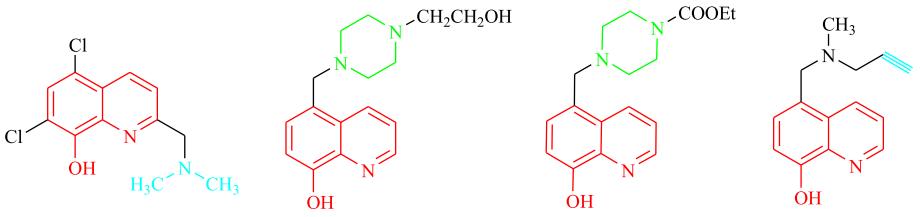

3 4 5 6

Fig. 3a Structural and anti-Alzheimer of 8-hydroxyquinoline analogs **3**–**6**.

showed a reduction in amyloid precursor protein (APP) expression and Aβ peptide secretion, with simultaneous activation of α-secretase and release of the neuroprotective neurotrophic solution APP alpha; therefore, **6** is a potential agent for the treatment of AD (Fig. 3a)(Gal, et al., 2005; Prati, et al., 2016). The above studies confirmed that 8-hydroxyquinoline is a strong iron chelator with antioxidant, anti-PD and anti-AD properties. In addition, they also found that a piperazine moiety can enhance the biological property, penetration propargyl moiety is an APP or protein regulation and processing to soluble APP alpha.

To search for and discover compounds with strong anti-Alzheimer activity, Prati et al. (Prati, et al., 2016) have synthesized two classes of 8-hydroxyquinoline derivatives and investigated their inhibition of human cholinesterase (*h*ChE). The results showed that the two series of compounds were not active, or weaker inhibitors, than *h*AChE (inhibition rate: 9.0 %–63.8 % for 5-chloro-8-hydroxyquinoline derivatives), but showed a dramatic inhibitory effect on human butyrylcholinesterase (*h*BChE) (49.2 %–89.1 % for 8-hydroxyquinoline compounds) at 40 μM. A comparison of compounds **7a** and **7b** indicated that the Cl atom on the benzene ring had a deleterious effect, removal of the Cl atom resulted in a fourfold increase in the inhibitory activity (with IC_{50} values from 23.3 to 5.71 μM). The compound with the highest anti-*h*BChE activity was **7a**. Compound **7c** with a bromine substitution also showed good BChE inhibition. Compound **7b** had anti-BChE, anti-aggregation, and Cu^{2+} and Zn^{2+} complexing properties *in vitro*, and may be worthy of further study (Fig. 3b). The study found that BChE inhibition was influenced by the presence, position of a substituent on the benzyl moiety, with the most potent compounds bearing a substituent at position 2. Yang et al. (Yang, et al., 2018) have synthesized two groups of analogs, **8** and **9,** with an 8-hydroxyquinoline containing a piperazine ring and evaluated their anti-AD activity. Eight compounds in series **8** and four compounds in series **9** had $A\beta_{1\text{-}42}$ aggregation inhibition activities from 32.46 % to 73.41 %, which were better than that of clioquinol (25.72 %) at 10 μM. Compound **8a** with a 2,4-difluorobenzene ring (IC_{50} = 5.05 μM) showed the strongest $A\beta_{1\text{-}42}$ aggregation inhibition activity. Compounds **8b** and **9a** (IC_{50} = 7.35 and 5.64 μM, respectively) with a 2-chlorobenzene ring displayed better inhibitory effects against $A\beta_{1\text{-}42}$ aggregation than resveratrol (IC_{50} = 12.43 μM). In addition, an F or Cl substituent at the 2-position of the aromatic ring for in series **8** compounds was beneficial for the inhibitory effect. A methoxyl substituent was detrimental for the inhibition. Compound **9a** could chelate biometals and inhibit Cu^{2+}/Zn^{2+}-induced $A\beta_{1\text{-}42}$ aggregation (Fig. 3b).

Wang et al. (Wang, et al., 2014a) have reported seven 8-hydroxyquinoline analogs containing piperidine ring as cholinesterase (ChE) inhibitors. Two compounds **10a** (n = 3 in the linker) and **10b** (n = 2 in the linker) (**10a**: esterase acetylcholinesterase (*ee*AChE), IC_{50} = 2.7 μM and *eq*BuChE, IC_{50} = 4.5 μM) and (**10b**: *ee*AChE, IC_{50} = 1.8 μM and *eq*BuChE, IC_{50} = 1.6 μM) displayed better inhibition activity.

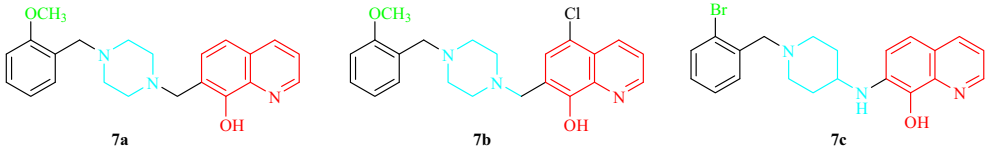

	7a	7b	7c
*h*AChE Inhib.[%]	NA	21.9	55.9
*h*BChE Inhib.[%]	89.1	63.9	77.2
*h*BChE IC_{50} (μM)	5.71	23.3	11.4

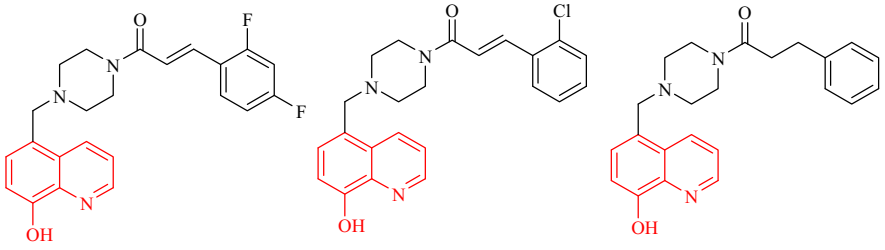

	8a	8b	9a
$A\beta_{1\text{-}42}IC_{50}$ μM	5.05	7.35	5.64

Fig. 3b Structural of 8-hydroxyquinoline analogs including with piperazine, piperidine ring **7**–**9**.

However, **10b** exhibited the best activity profile of all the compounds investigated. The SAR analysis showed (1) a trend was detected with α-aminonitrile series, linker length, α-aminonitriles compounds proved to be more potent than amines at inhibiting both enzymes; (2) bearing no methyl in linker connecting N-benzyl-piperidin-4′-yl residue to the N-propargyl core was inactive; (3) regarding tertiaryamines effect at inhibiting both ChE increased from n = 1 to n = 3. Molecular modeling of eeAChE and eqBuChE with **10b** R- and S-enantiomers indicated —CN group formed a hydrogen bond of side chain of Asn83 for R-enantiomer, this bond was bifurcated in the case of S- enantiomer; the hydrophobic interactions with the catalytic triad residues of Ser198 and His438 were found in this orientation. In mode B, only one hydrogen bond was observed for R-enantiomer, it was formed between —CN and —OH group of Thr120, S-enantiomer —OH group of quinoline ring established a hydrogen bond with the catalytic triad residue His438 (Fig. 3c). In 2015, Knez et al. (Knez, et al., 2015) reported the preparation and ChE inhibitory activity and anti-aggregation effects of a family of nitroxoline-based analogs with an 8-hydroxyquinoline scaffold. Six analogs displayed *h*BChE inhibitory activity and compounds **11a** and **11b** exhibited good inhibitory effects with the IC_{50} values of 2.14 and 0.215 μM, respectively. The SAR analysis was shown all the synthesized derivatives had weaker *h*BChE inhibitory activity compared with the lead compound. The derivatives with benzoxazole or benzothiazole skeletons were active when the alkalinity of the piperidine nitrogen was retained, and when the compounds had a methylene group linkage between the aromatic bicyclic and piperidine structures. In addition, **11b** had promising selective Cu^{2+}-chelation properties. In the crystal structure, the 5-NO_2-quinolin-8-ol moiety of **11b** was located in the acyl-binding pocket of the *h*BChE active site. Molecular modeling of **11b** BuChE indicated the hydroxyl group of the nitroxoline was hydrogen bonded to the His438 ε-imidazole nitrogen, and the OH group on the quinoline nitrogen formed a hydrogen bond with Ser198. The NO_2 group interacted with the carbonyl groups of the residues Ser287 and Phe285 (Fig. 3c).

In 2018, Wang et al. (Wang, et al., 2018b) synthesized a family of quinoline-indole analogs as multi-target-directed ligands for AD therapy. Four classes of analogs were synthesized and compounds **12a** (X = H, R_1 = OH) (inhibition, 51.2 %) and **12b** (X = Cl, R_1 = OH) (inhibition, 66.8 %) exhibited better activity than clioquinol (1.9 %) and melatonin (19.3 %) (Fig. 3d). Compound **12b**, a metal chelator, which had a neuroprotective effect with antioxidant activity in cells with an median effective concentration (EC_{50}) value of 0.1 μM, a 71.6 % and 85.8 % reduction in of self- or Cu^{2+}-induced Aβ-aggregation, and 72.7 % and 83.3 % disintegration of prefabricated self- or Cu^{2+}-related $A\beta_{1-42}$ aggregate fibrils, displayed the best anti-AD activity of all the tested compounds. The SAR analysis of the inhibitory effect on $A\beta_{1\text{-}42}$ self-induced aggregation for these analogs showed: (1) in presence of a Cl-atom on oxine moiety of quinoline ring played a pivotal role in the inhibitory activity; (2) methylation of the hydroxyl group or cyclization with methoxy group seemed unfavorable for the effects on quinoline ring; (3) it demonstrated that phenolic hydroxyl group on indole moiety was preferable for inhibitory activity. In 2020, Fernández-Bachiller et al. (Fernández-Bachiller, et al., 2010) have synthesized a class of tacrine-8-hydroxyquinoline analogs as multi-target-directed ligands for AD therapy (Fig. 3d). Compounds 1**3a**, 1**3b**, and 1**3c** inhibited *h*AChE with IC_{50} values of 0.5–5.5 nM and inhibited *h*BuChE with IC_{50} values of 6.5–55 nM. Compound **13b** displayed the best *h*AChE

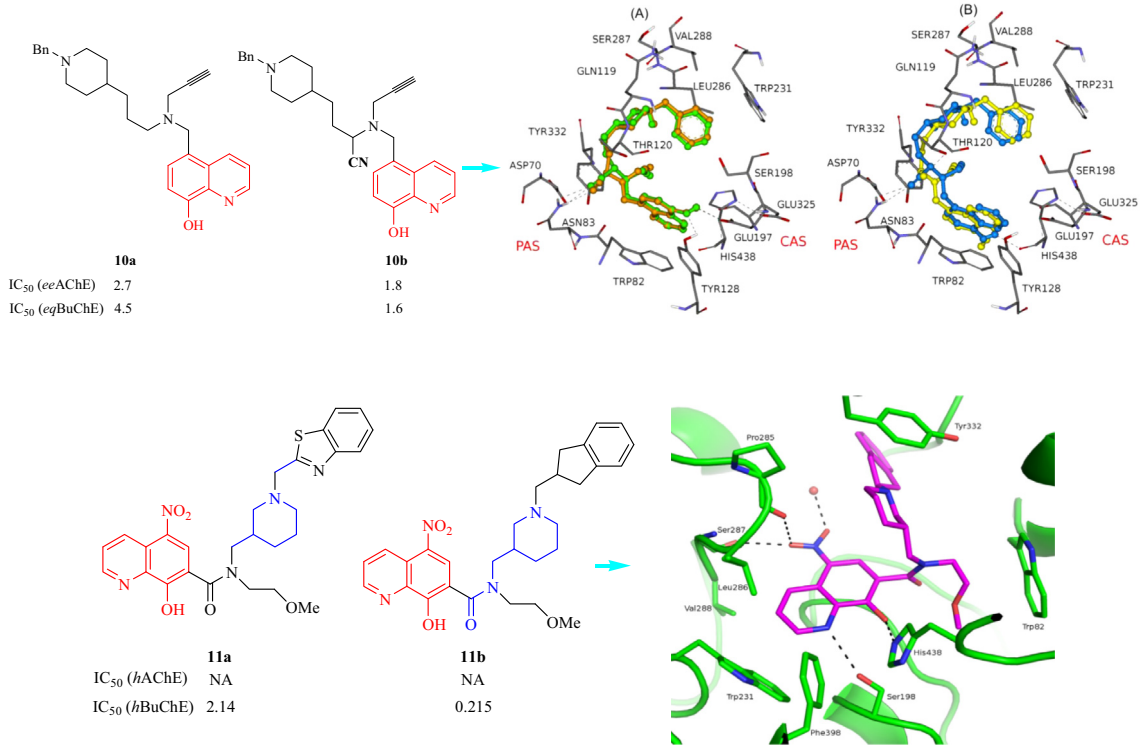

Fig. 3c Structural of 8-hydroxyquinoline analogs (**10,11**) containing piperidine ring.

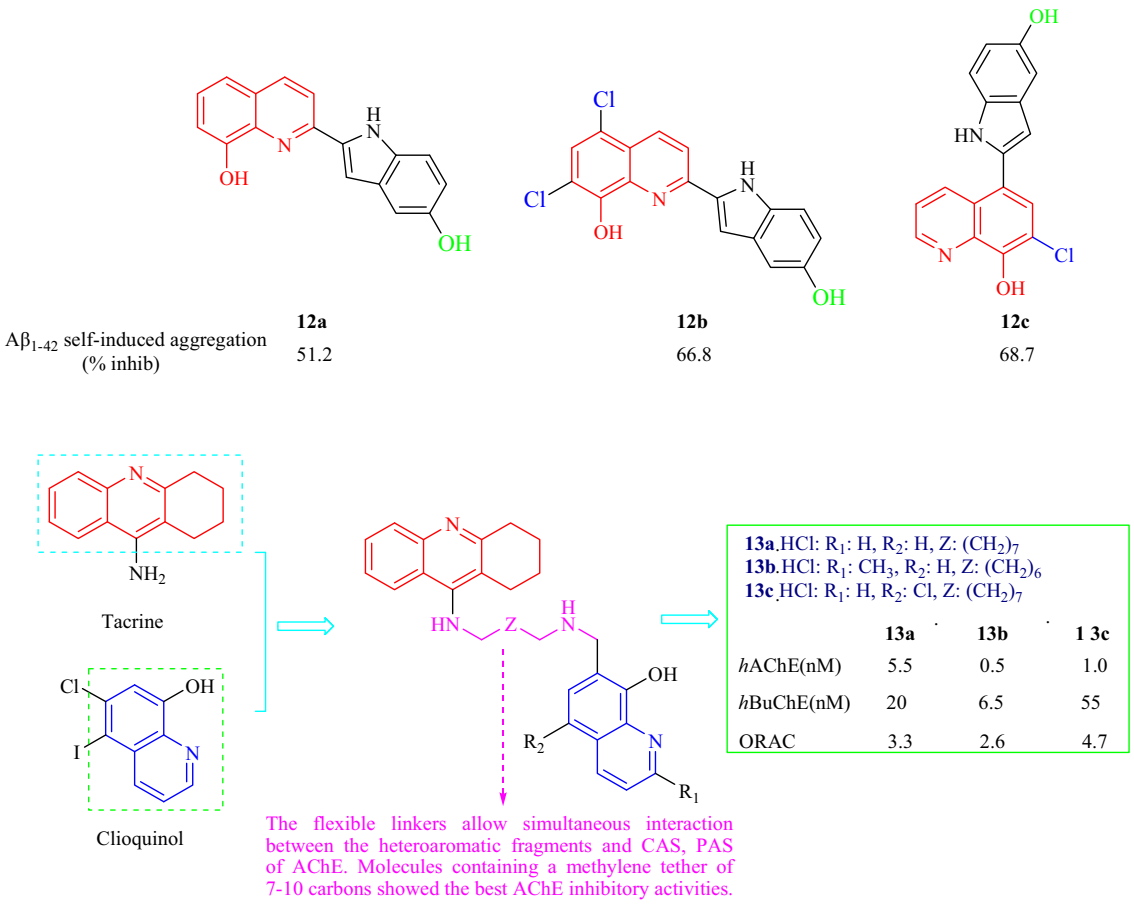

Fig. 3d Structural of 8-hydroxyquinoline analogs (**12,13**) containing indole and tacrine ring.

inhibition of the tested compounds with 700 times higher activity compared with tacrine, and 1**3a** also showed good antioxidant properties, being 3.3 times more potent than V_E in oxygen-radical absorbance capacity. In the propidium displacement assay, 1**3a**, 1**3b**, and 1**3c** could reduce Aβ-aggregation through AChE by 22 %, 19 %, and 27 %, respectively, at a concentration of 0.3 μM. The three compounds could selectively complex Cu^{2+} and penetrate the central nervous system (CNS). The results displayed Clloquinol for its metal-chelating, neuroprotective, antioxidant properties. Molecules containing an unsubstituted 8-hydroxy quinoline fragment displayed the best AChE inhibitory effects. Tacrine for the inhibition of ChE through its binding to the CAS.

Fiorito et al. (Fiorito, et al., 2013) have synthesized a family of quinoline analogs and assessed the phosphodiesterase 5 (PDE5) inhibition. The compounds maintained a CN group at the C7-position, a $–CH_2OH$ group at the C3-position, and the benzylamino moiety of the quinoline ring, because these factors have been shown to be important for PDE5 activity and selectivity (Fig. 4) (Bi, et al., 2004). In the biological analysis, six compounds with substituents at the C8-position showed PDE5 inhibition with IC_{50} values from 0.27 to 15.0 nM, the effect of the substituents was in the order of cyclopropyl > $-N(CH_3)_2$ > morpholinyl > –NH-cyclopropyl > $–NH(CH_2)_2N(CH_3)_2$ > $–NH(CH_2)_2$. Among these compounds, compounds **14a**, **14b**, and **14c** showed good phosphodiesterase inhibition (PDEI) activity. In addition, **14a** and **14b** also showed selectivity toward all 11 PDEs. The selectivity of **14a** and **14b** toward PDE6 and PDE11 was higher than that of sildenafil, vardenafil, ortadalafil. The results indicated that **14a** elicited effects by which impairments in synaptic plasticity and memory were rescued by elevated levels of $Aβ_{42}$. Therefore, **14a** is a potential PDE5I for the treatment of AD. In 2013, Silva et al. (Silva, et al., 2013) prepared a class of quinolinodonepezil analogs and assessed the AChE and BuChE inhibition. Two quinolinodonepezil compounds, **15b** and **15c**, were more potent inhibitors of *ee*AChE than *h*AChEas shown in Fig. 4. **15a** did not have inhibitory activity. **15b** and **15c** were inactive against *eq*BuChE and were more potent inhibitors of *h*BuChE than *eq*BuChE. The *N*-benzylpiperidine unit was thought to be important for *ee*AChE inhibition as it was the main element involved in the binding to AChE. Pudlo et al. (Pudlo, et al., 2014) have designed and synthesized two families of 1,2-dihydroquinoline-3-carboxamides linked to benzylpiperidines as AChE inhibitor for AD (Fig. 4). In the first series, when R_2 was hydroxyl, the order of activity for the anti-AChE inhibitory effect was nBu > Me > H (n = 0 or 1) and when R_2 was hydrogen, the order of activity was Me (n = 1) > Me (n = 0) > Ph; an NH_2 group (**16b**: $R_2 = NH_2$, $R_1 = CH_3$) had an effect similar to the OH group (**16a**: R_2 = OH, $R_1 = CH_3$). In the second series, compounds had 6,7-di-OCH_3or 6,7-di-OH groups

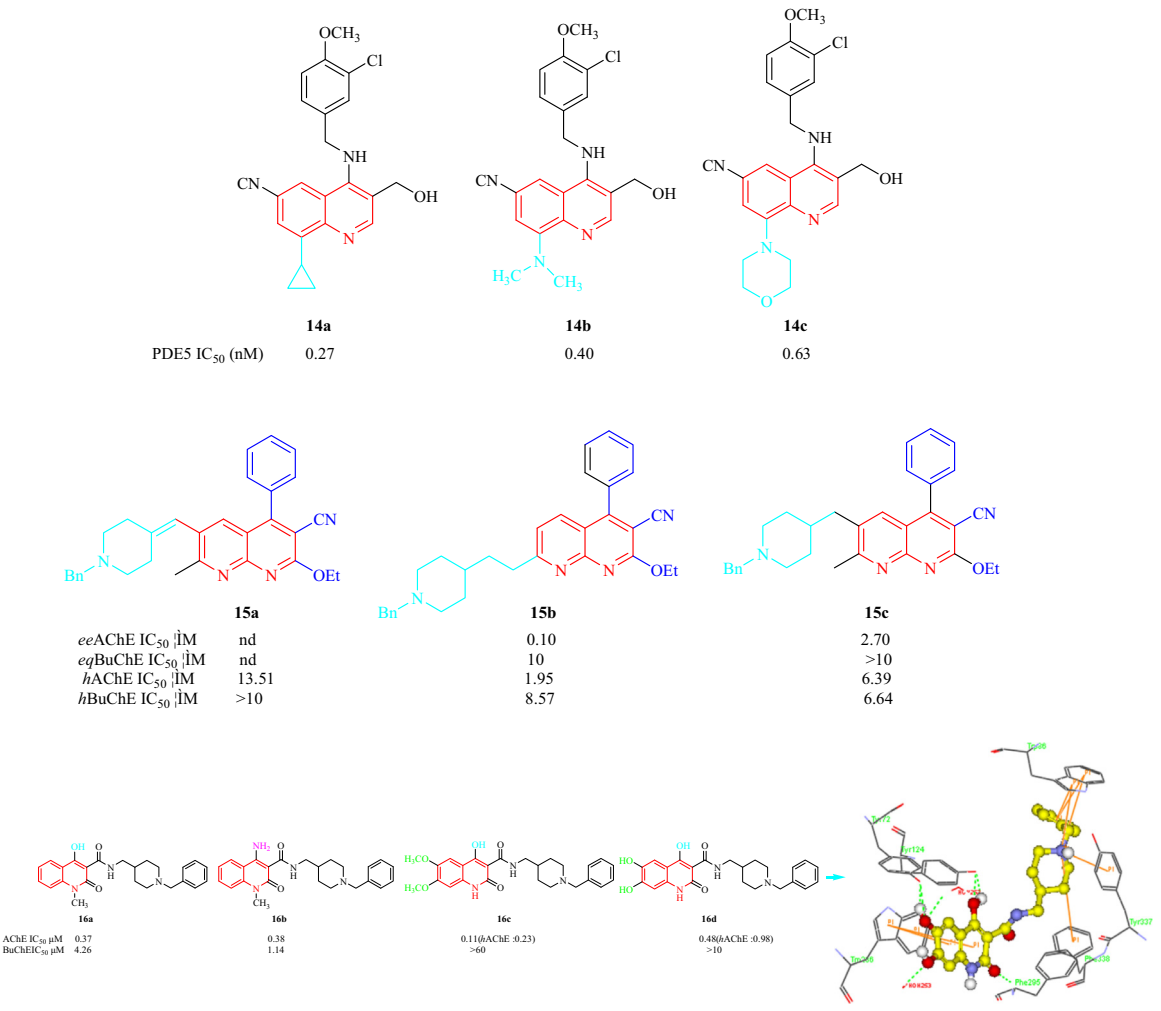

Fig. 4 Structural and anti-Alzheimer of quinoline and related analogs **14**–**16**.

on the quinolone ring, and **16c** (R_1 = H, R_3 = OMe) exhibited the most inhibition of AChE with an IC_{50} value of 0.11 μM, but even at 60 μM there was no observed inhibition of BuChE. However, **16d** (R_1 = H, R_3 = OH), the *O*-demethylated derivative, inhibited AChE with an IC_{50} value of 0.48 μM. No BuChE inhibition was displayed at 10 μM. **16c** and **16d** also showed *h*AChE inhibition with IC_{50} values of 0.23 and 0.98 μM, respectively. The SAR analysis displayed: (1) with a methylene linkage (n = 1) between piperidine ring and *N*-amide present a higher effect than compounds without spacer (n = 0); (2) AChE inhibition increases when *N*-quinoline is substituted; (3) an amino group has similar activity than a hydroxyl group at 4 position on the quinoline ring. The molecular modeling of **16d** *h*AChE indicate piperidinium is snaking along gorge, making cation π interactions with aromatic rings in Tyr337 and even less in Phe338. The quinolone moiety is linked to peripheral anionic site by π-stacking interactions with Trp286, an H-bond between hydroxyl group in position 4 of quinolone and a hydroxyl of Tyr124 and another one between carbonyl in position 2 of quinolone and a NH of Phe295.

In 2015, Wang et al. (Wang, et al., 2015c) have reported the synthesis of a class of 2-arylethenylquinoline analogs as multi-target drugs for AD. Most of the analogs displayed $A\beta_{1\text{-}42}$ aggregation inhibition from 23.6 % to 83.9 % at 20 μM. Of these compounds, **17a**, **17b**, and **17c** possessing piperazine or piperidine ring at 4-position on quinoline ring displayed the most potent inhibitory effect on $A\beta_{1\text{-}42}$ aggregation with inhibitory rates of 81.7 %, 83.9 %, and 81.8 %, respectively, and IC_{50} values of 10.8, 9.7, and 10.3 μM, respectively, which was greater inhibitory activity than resveratrol (IC_{50} = 11.4 μM) (Fig. 5). In addition, **17b** (IC_{50} = 64.0 ± 0.1 μM for AChE and IC_{50} = 0.2 ± 0.1 μM for BuChE), and **17c** (IC_{50} = 68.3 ± 0.1 μM for AChE and IC_{50} = 1.0 ± 0.1 μM for BuChE) displayed a good ChE inhibitory effect, with high selectivity toward BuChE. Furthermore, **17b** was a selective metal chelator for Cu^{2+} and Fe^{2+}. He et al. (He et al., 2017) and Safarizadeh and Garkani-Nejad (Safarizadeh and Garkani-Nejad, 2019) have also studied this series of analogs and their results supported the above conclusions. The SAR indicated flexible amino at 4-postion of quinoline scaffold contributed to the increased activity, substituent group with 4-dimethylamino or 4-diethylamino on benzene ring is favorable for inhibitory activity of $A\beta_{1\text{-}42}$ aggregation. In 2018, a family of flexible amino-2-arylethenylquinoline analogs was prepared and investigated as multi-target agents for the treatment of AD by Wang et al. (Wang, et al., 2018d). All the derivatives displayed strong inhibition of $A\beta_{1\text{-}42}$ self-induced aggregation (> 77 % at 20 μM), which was similar to resveratrol (77.2 % at 20 μM).

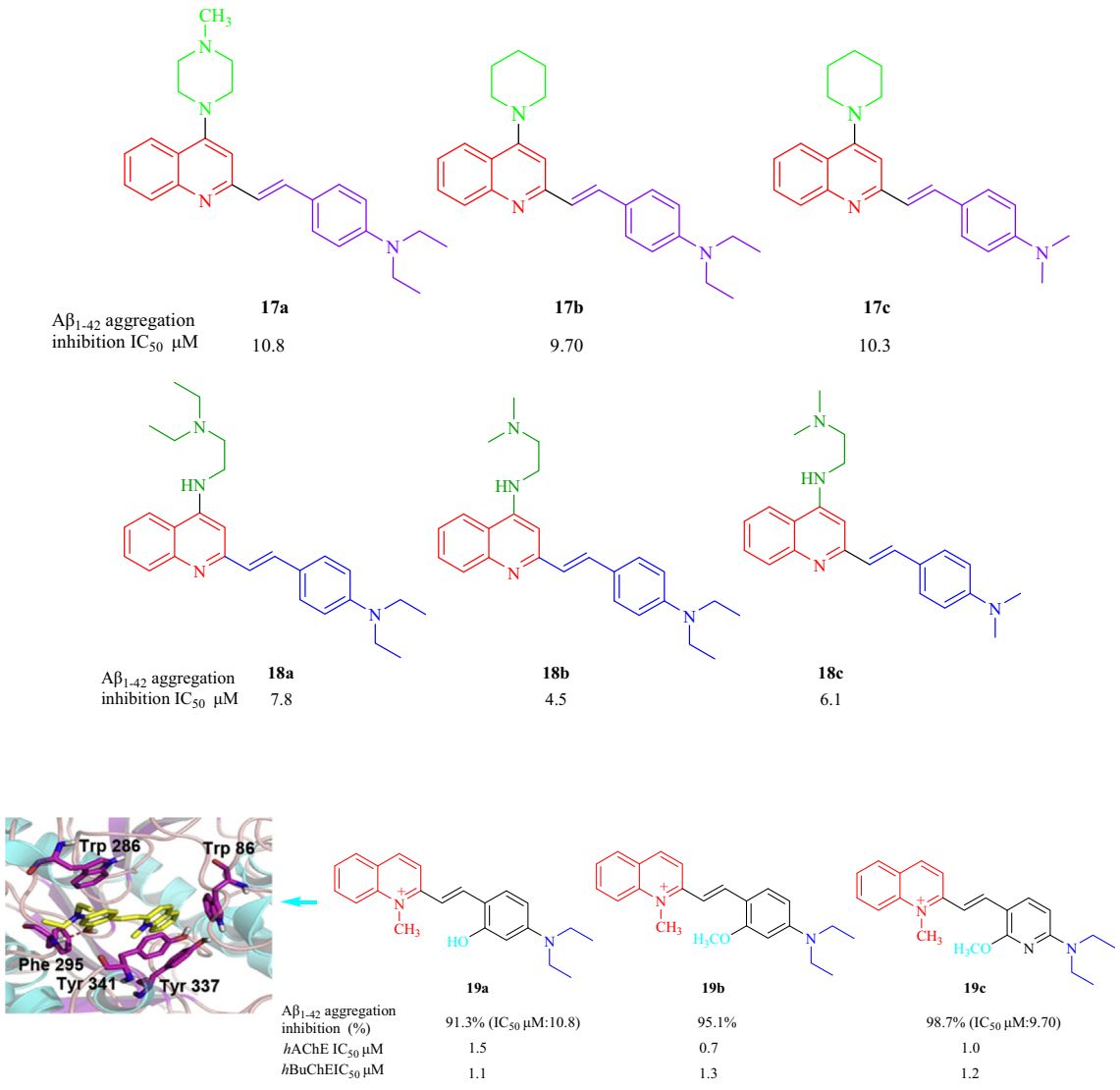

Fig. 5 Structure of 2-arylethenylquinoline derivatives **17**–**19.**

Compounds **18a**, **18b**, and **18c** (Fig. 5) showed good inhibitory effects with inhibitory rates of 95.3 %, 92.1 %, and 90.2 %. **18b** could effectively inhibit Cu^{2+}-induced $A\beta_{1\text{-}42}$ aggregation, had a protective effect on SH-SY5Y (human neuroblastoma cell) cytotoxicity induced by $A\beta_{1\text{-}42}$ without evident toxicity, and reversed the memory impairment of mice in a model of AD. Xia et al. (Xia, et al., 2017) have designed and synthesized 27 2-arylethenyl-*N*-methylquinolinium analogs and evaluated the Aβ-aggregation inhibition, ChE inhibition, and antioxidant effect. The results showed that 19 compounds displayed Aβ-aggregation inhibitory activity with $A\beta_{1\text{-}42}$ aggregation inhibition from 50.1 % to 98.7 %. Compounds **19a**, **19b**, and **19c** showed the greatest inhibitory activity (91.3 %, 95.1 %, and 98.7 %, respectively, at 20 μM) of all the compounds (Fig. 5). In addition, most compounds displayed similar or weaker inhibitory activity toward *h*AChE than tacrine and donepezil. **19a**, **19b**, and **19c** displayed better *h*AChE inhibitory activity, compared with tacrine and donepezil, with IC_{50} values of 1.10, 1.30, and 1.20 μM, respectively. In summary, the SAR of this series of derivatives implies (1) the flexible amino at 4-postion of quinoline scaffold contributed to the increased activity; (2) the substituent group with 4-dimethylamino or 4-diethylamino on benzene ring is favorable for the inhibitory activity. Molecular modeling was performed to investigate the binding mode between **19a** and *h*AChE displayed the *N* atom on quinoline ring interacted with Tyr337 and Tyr341 via π-cationic interactions. A hydrogen bond formed between the hydroxyl and acyl groups of phe295 in the phenyl ring **19a** binding pocket (Fig. 5).

Rodríguez et al. (Rodríguez, et al., 2016) have synthesized a series of *N*-allyl/propargyl-4-substituted-1,2,3,4-tetrahydro-quinoline analogs and investigated the AChE and BChE inhibitory activity. The synthesized compounds had poor activity against AChE and BChE. The *N*-allyl-tetrahydroquinolines displayed inhibition of both AChE and BChE enzymes, with more inhibitory activity against BChE than AChE. The order of activity against BChE was 6-CH_2CH_3 > 6-Br > 6-CH_3 > 6-OCH_3 > 6-Cl > 6-F > 6-H; compounds **20a**, **20b**, and **20c** (IC_{50} values of 31.66, 25.58, and 29.08 μM, respectively) had better inhibitory effects toward BChE than the other tested compounds. However, *N*-propargyl-tetrahydroquinolines exhibited weak inhibition against AChE

with IC_{50}values from 259.63 to 661.38 μM. A molecular docking study indicated that **20b** had a π-π stacking interaction with residue Trp82 within the BChE active site (Fig. 6). In 2017, Sang et al. (Sang, et al., 2017) designed and synthesized 33 3,4-dihydro-2(1*H*)-quinoline-*O*-alkylamine derivatives and evaluated their multifunctional biological effects. All the derivatives displayed moderate to good inhibition of *ee*AChE with IC_{50} values from 0.56 to 23.5 μM, and showed similar potencies against *eq*BuChE with IC_{50} values from 0.87 to 39.6 μM. Three compounds **21a**, **21b**, and **21c** showed good inhibition of AChE with IC_{50} values of 0.90, 0.76, and 0.56 μM, respectively. **21c** exhibited the most potent activity against AChE and had an IC_{50} value of 2.3 μM against BuChE. SAR indicated piperazine substituent exhibited better inhibitory effects, AChE and BuChE inhibitory activity increased with an increase in methylene chain length. In addition, with isopropylpyrazine group and six methylene chain indicated the best AChE inhibitory activity. The molecular modeling studies displayed 4-benzylpiperidine of moiety of **21c** bind to Try334, the long chain of methylene interacted with Phe330 and Tyr121 by hydrophobic interaction, carbonyl group and NH at quinoline nucleus bind to Trp84 and Ser124 intermolecular hydrogen bonds. In 2021, Bautista-Aguilera et al. (Bautista-Aguilera et al., 2021) have synthesized 19 quinolinones and 13 dihydroquinolinonesas potential multi-target drugs for the treatment of AD. None of the compounds inhibited human recombinant MAO. Three analogs displayed promising *h*AChE and *h*BuChE inhibition **22a** (IC_{50} = 0.29 and 12.73 μM, respectively), **22b** (IC_{50} = 0.96 and 6.70 μM, respectively), and **22c** (IC_{50} = 1.58 and 16.73 μM, respectively) (Fig. 6). The SAR suggested isopropylpiperazine seemed also essential for the *hr*AChE activity with the butoxy group as the optimal linker between the core and basic centre. The molecular modeling of **22a** *h*AChE indicated oxygen ether formed a hydrogen bond with Gly121 in the oxyanion hole, while Tyr124 formed a hydrogen bond with the hydrogen of one of the quaternized nitrogen of the piperazine moiety, carbon hydrogen interactions were observed between the ligand and Thr83, Tyr124, Ty337.

In 2018, Umar et al. (Umar, et al., 2018) designed and synthesized seven 4-[(7-chloroquinolin-4-yl)oxy]-3-ethoxybenzalde hyde derivatives and evaluated the Aβ-aggregation inhibition, anti-oxidation, and metal chelation effects. Most of the compounds inhibited self-mediated $A\beta_{1\text{-}42}$ aggregation ranging from 30 % to 53.72 % and compounds **23a** and **23b** (Fig. 7) displayed the most inhibition with values of 53.73 % and 53.63 %, respectively, at 50 μM. **23a** and **23b** also inhibited *h*AChE activity with values of 47.36 % and 58.26 %, respectively, which were higher than donepezil (23.66 %). The SAR suggested the quinolinone core looked more potent than

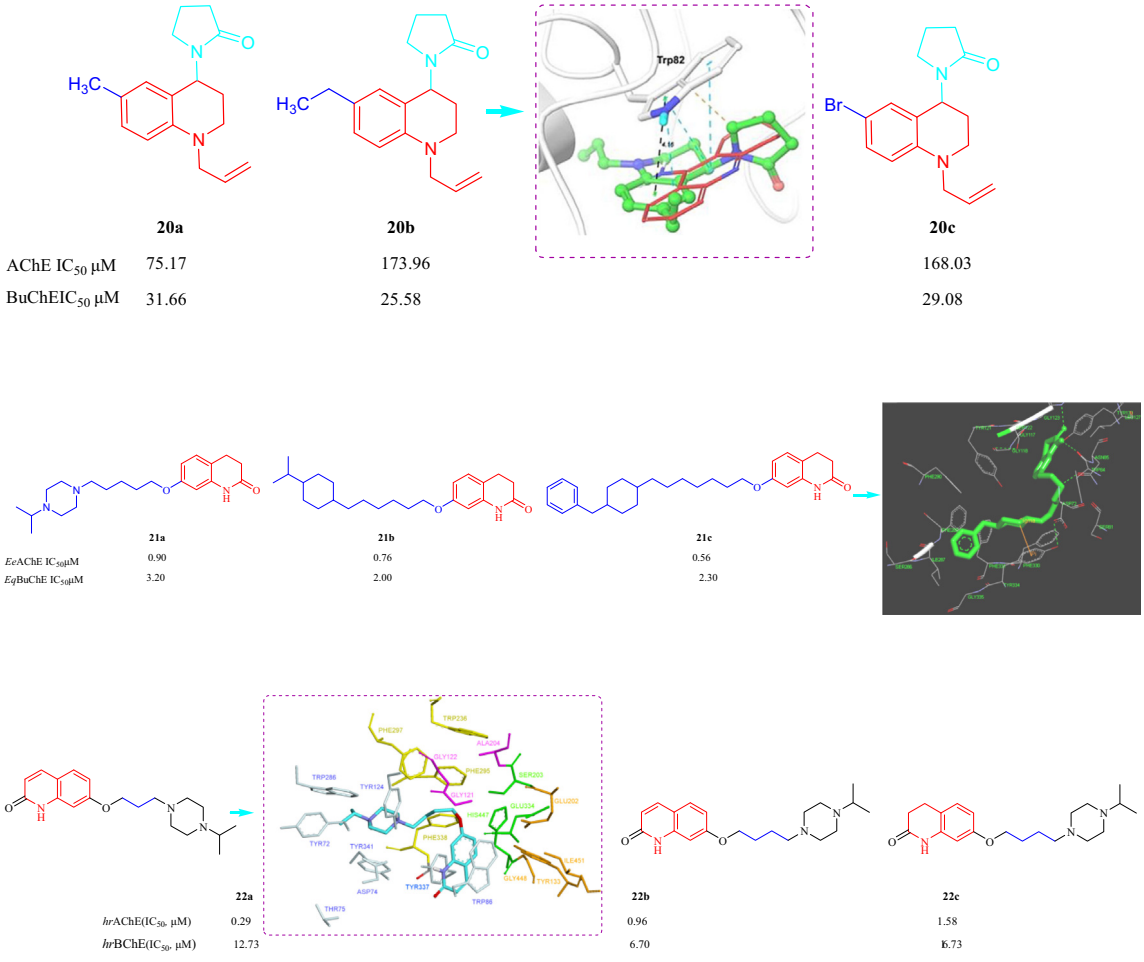

Fig. 6 Structure of tetrahydro-quinoline and their derivatives **20**–**22.**

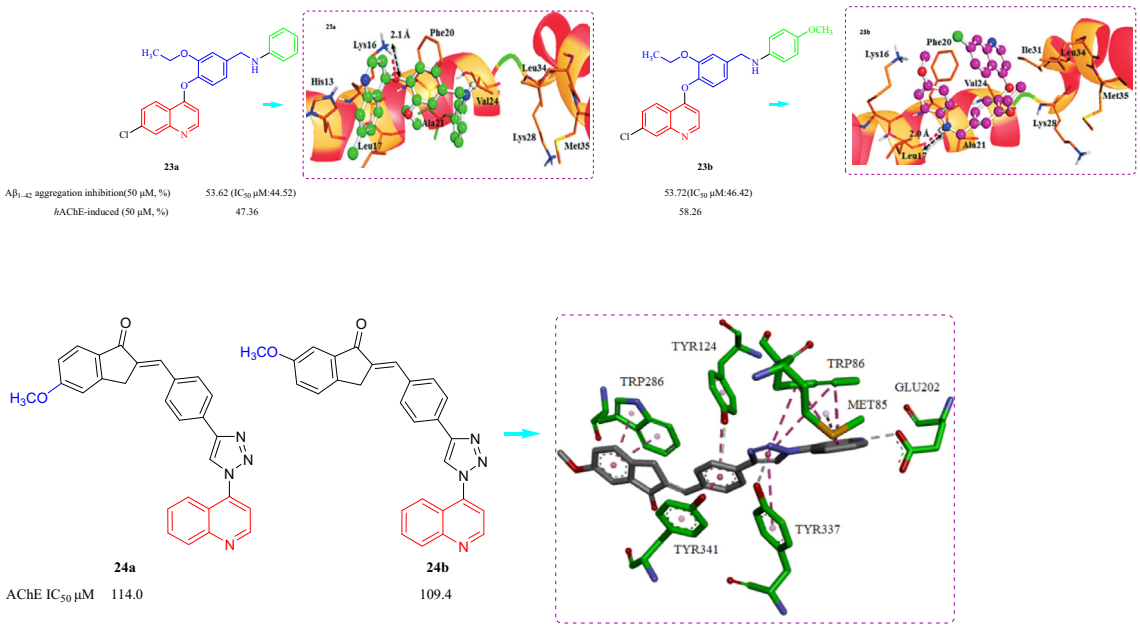

Fig. 7 Structure of quinoline and their derivatives **23, 24.**

the semiunsaturated dihydroquinolinone as *hr*AChE inhibitor, with electron donating groups like methyl, methoxy displayed higher potency while those with electron withdrawing groups like fluorine. The molecular modeling of **23a** and **23b** *h*AChE indicated an intermolecular hydrogen bond interaction was formed between *O*-atom for **23a** attached to quinoline group and backbone NH_2 group of Lys16. While an intermolecular hydrogen bonding interaction was observed for **23b** between –NH group and carbonyl group of Leu17. In 2016, Mantoani et al. (Mantoani, et al., 2016) reported the preparation and assessment as *h*AChE and *h*BChE inhibitors of a class of tacrine-donepezil derivatives. The results are presented in Fig. 7, four compounds inhibited *h*AChE with IC_{50}values from 109.4 to 146.6 μM. Among the tested compounds, compounds **24a** and **24b** showed the best inhibition against *h*AChE with IC_{50} values of 114.0 and 109.4 μM, respectively. The tested compounds did not display an inhibitory effect against *h*BChE. The binding mode for the docking of the inhibitor **24b** with *h*AChE displayed π-π stacking interaction between the indanone ring of **24b** with TRP286, and a second π-π stacking interaction between benzyl group with aromatic tyrosine residues Tyr124, 337 and 341.

Bosak et al. (Bosak, et al., 2019) also studied eight 4-aminoquinoline derivatives with different substituents, and investigated the *h*AChE and *h*BChE inhibition. All the tested compounds exhibited slight selectivity toward *h*AChE (with K_i constants from 0.46 to 11 μM) over *h*BChE, and compounds **25a**, **25b**, and **25c** showed the highest affinity toward *h*AChE with K_i values of 0.46, 0.61, and 0.77 μM, respectively (Fig. 8). The SAR analysis showed that the replacement of chlorine and trifluoromethyl group on C(7) displayed strong AChE inhibition activity. It represented with long alkyl chain or adamantyl group on C(4)-amino group, is important for achieving high inhibition potency. The molecular modeling of **25a** *h*AChE indicated to stabilize with residues Tyr124, Trp286, and Tyr341 in AChE, and protonated amino group was stabilized with Trp86 and Glu202 in AChE. In 2019, to simplify the structure of the hybrid product, Mo et al. (Mo, et al., 2019) designed and synthesized a series of quinoline-ferulic acid hybrids and evaluated the ChE inhibition. Most compounds displayed good inhibitory effects toward both AChE and BChE. Among them, **26a** was found to be the most potent inhibitor against AChE (IC_{50} = 0.62 ± 0.17 μM) and **26b** was the most potent inhibitor against BChE (IC_{50} = 0.10 ± 0.01 μM, Fig. 8). **26a** and **26c**, as representative compounds, were shown to be competitive inhibitors of AChE and BChE. SAR indicated incorporating a three-carbon chain or a four-carbon chain exhibited to enhance AChE and BChE inhibitory effects; the quinoline-cinnamic acid hybrids compared to quinoline-ferulic acid hybrids showed similar effects and target selectivity; compound with 2-methyl substitued on quinoline ring showed to enhance AChE and BChE inhibitory effects. The molecular modeling of **26a** AChE indicated *N*-atom on quinoline ring interacts with Ser125 by a hydrogen bond, benzyloxyl moiety interacts with Leu289 through a π-alkyl contact, ethylene diamine linker shows van der Waals interactions with Tyr341, Asp72. For **26b** in the active site of BChE displayed *N*-atom interacted with Asp70 by a salt bridge, carbonyl group of the cinnamic acid moiety forms a hydrogen bond with His438. A series of 4-*N*-phenylaminoquinolines derivatives were prepared and the inhibitory effects on AChE and BChE were assessed by Zhu et al. (Fig. 8) (Zhu, et al., 2019a). All the synthesized compounds inhibited AChE (IC_{50} values of 0.65–11.84 μM). The two analogs **27a** and **27b** inhibited AChE and BChE with IC_{50} values of 0.86 and 2.65 μM, respectively (**27a**) and 2.65 and 2.78 μM, respectively (**27b**). **27a** displayed the best effect against both AChE and BChE. The SAR analysis indicated the order of inhibitory potency against AChE: *meta* ≥ *ortho* > *para* on the substituted position in the 4-*N*-phenyl ring, while *para*-substituted compounds were clearly less potent against BChE than *meta*-substituted or *ortho*-substituted ones. The molecular

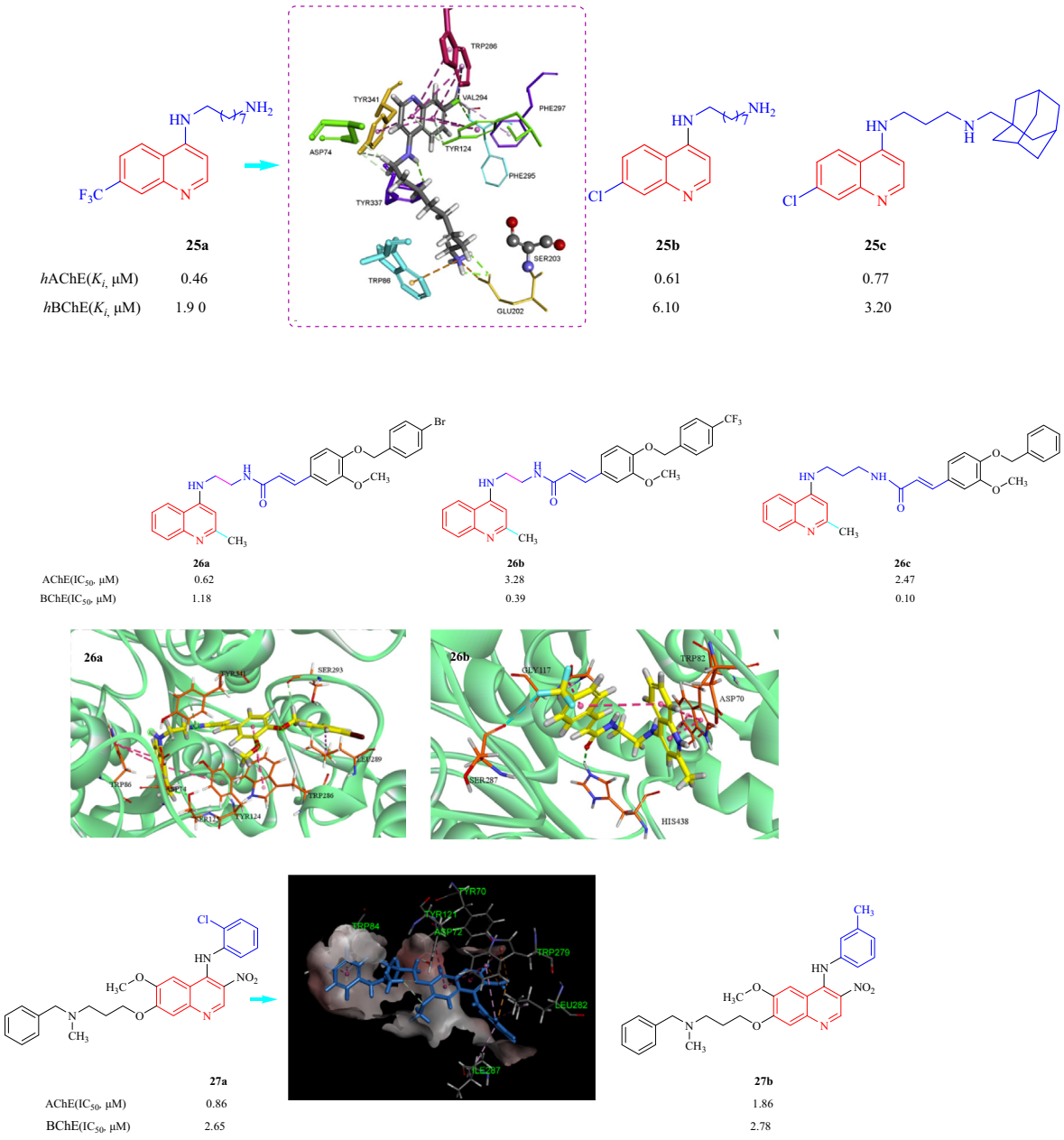

Fig. 8 Structure of 4-aminoquinoline quinoline, 4-*N*-phenylaminoquinoline derivative **25**–**27**.

modeling of **27a** AChE indicated a π-alkyl interaction between the 4-*N*-phenyl ring and *sec*-butyl moiety of Ile287, *N*-methylbenzylamine fragment interacted with CAS by π-π-stacked interaction with Trp84, quinoline moiety made a carbon hydrogen bond with Tyr70.

In 2020, Fu et al. (Fu, et al., 2020) reported a family of quinolinone analogs bearing a dithiocarbamate as multifunctional AChEIs to treat AD. Most compounds displayed strong selective inhibition of *ee*AChE, and good selectivity for *ee*AChE over *eq*BuChE. Compound **28a**, which had a four carbon linker and a piperidine at the terminal position showed the most effect against *ee*AChE and *h*AChE (IC_{50} = 0.22 and 0.16 μM, respectively). **28b** with di-CH_3 groups on the coumarin ring also inhibited *ee*AChE and *h*AChE (IC_{50} = 0.34 and 0.39 μM, respectively) (Fig. 9). The SAR analysis indicated including a four-carbon atom linker showed better inhibitory effect; the replacement of piperidine group using other cyclic amines were not beneficial for AChE inhibition. The molecular modeling of **28a** for AChE indicated piperidine group established a 'arene-H' interaction with Trp 86, the polymethylene chain was folded in a conformation to make it interact with mid-gorge site by a 'arene-H' interaction with Tyr 341. In 2021, Zaib et al. (Zaib, et al., 2021) reported a class of quinoline-thiosemicarbazone derivatives as inhibitors of ChE (Fig. 9). All the synthesized compounds were fully selective for AChE activity, with IC_{50} values ranging from 0.12 to 60.9 μM. Compound **29a** exhibited the greatest inhibitory effect (IC_{50} = 0.12 ± 0.02 μM), which was five times stronger than the positive control drug galantamine (IC_{50} = 0.62 ± 0.01 μM). The SAR analysis indicated that an ethylmorpholine

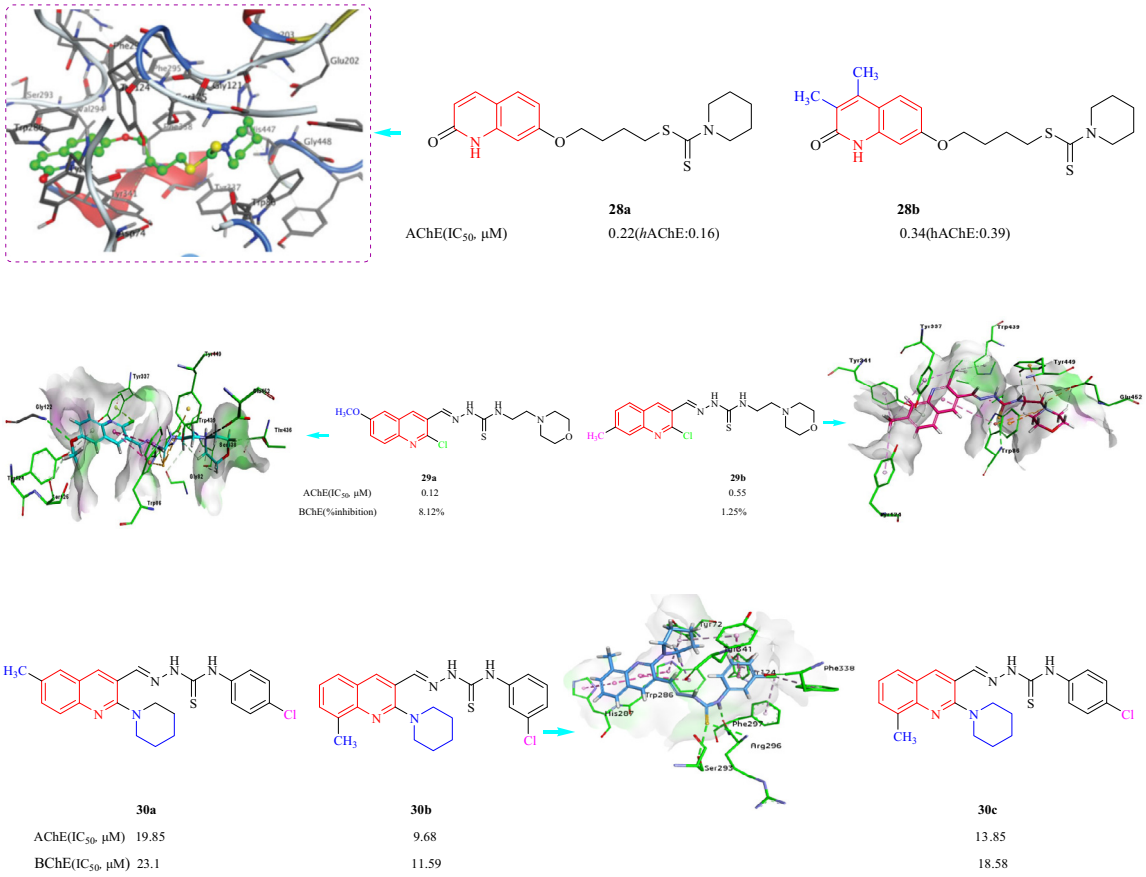

Fig. 9 Structure of quinolinone-dithiocarbamate and quinoline-thiosemicarbazone **28**–**30**.

group at the R_3 position on the thioamide unit resulted in better inhibition than a benzene ring; compounds with an ethylmorpholine were determined to be lead candidates. Moving –OCH_3 group from the six-position to the seven-position on the quinoline ring led to a reduction in the inhibition. The substitution of ethyl morpholine with a benzene ring was detrimental for the inhibition. All compounds showed < 50 % inhibition against BChE. The molecular docking of **29a** and **29b** analysis suggested the active pocket like π-π *T*-shaped by quinoline ring and π-sulfur by sulfur atom in thiosemicarbazone moiety with Trp86. the hydrogen bonding was noticed between oxygen atom and Gly122, nitrogen atom of morpholine ring exhibited interactions with Glu452 for **29a**. While for **29b**, nitrogen atom of morpholine ring was involved in formation of salt bridge and π-cation, interactions with Glu452 and Tyr449, respectively. Munir et al. (Munir, et al., 2021) have prepared a library of piperidine-containing quinolinyl thiosemicarbazones and investigated the AChE and BChE inhibition (Fig. 9). First, the effect of methyl substitution at the 6-(R_1) and 8-(R_2) positions of quinoline was studied while keeping the thiosemicarbazide chain unchanged. Five compounds displayed IC_{50} values < 20 μM (including **30a**, IC_{50} = 19.85 μM and **30c**, IC_{50} = 13.85 μM, against AChE). Compound **30b** showed the strongest inhibitory effect toward AChE and BChE (IC_{50} = 9.68 and 11.59 μM, respectively), when the 8-position of the quinoline was substituted with a methyl group, the anti-cholinesterase activity of the *meta*-substituted chlorine and fluorine derivatives was the greatest. Molecular docking studies of **30b** for AChE indicated two hydrogen bonds with sulfur and NH of carbothioamide by Arg296, a hydrogen bond with sulfur of thiocarbonyl by Ser293 (Fig. 9).

Maalej et al. (Maalej et al., 2012a) have designed and prepared a family of racemic tacrine analogs and studied the inhibition of *h*AChE and *h*BuChE (Maalej et al., 2011b). Compounds with electron-donating groups, such as 3-OCH_3-4-OH, 2,4-di-OCH_3, 4-OH, 2-OCH_3, or 4-CH_3 displayed good inhibitory effects with IC_{50} values from 0.33 to 0.40 μM. Analysis of the SAR indicated that R group substitutions on the benzene ring increased the inhibition in the order: H > 4-OH-3-OCH_3 > 2,4-di-OCH_3 > 4-CH_3 > 3,4,5-tri-OCH_3 > 2-OCH_3 > 4-OH. Compounds **31a** (IC_{50} = 0.30 ± 0.04 μM) and **31d** (IC_{50} = 0.33 ± 0.04 μM) showed activity against *h*AChE (Fig. 10a). Compounds bearing the electron-withdrawing groups 4-NO_2, 3,4-di-Cl, and 2,6-di-Cl were 13–19 times less potent than other compounds, the activity was in the following order: 2,6-di-Cl > 3,4-di-Cl > 4-NO_2, but were still selective *h*AChE inhibitors. Molecular modeling of *h*AChE with **31** *R*- and *S*-enantiomers indicated benzochromene moiety interacts with Trp286 and tetrahydroquinoline moiety interacts with Tyr341 via π-π stacking. The hydrogen bond interaction between hydroxyl substituent in the phenyl ring and hydroxyl group of Thr75 for *R*-, while *S*-enantiomers, hydroxyl group of Thr75 establishes hydrogen bond interactions with two oxygen atoms of methoxy and hydroxyl groups. Eghtedari et al. (Eghtedari, et al., 2017) have

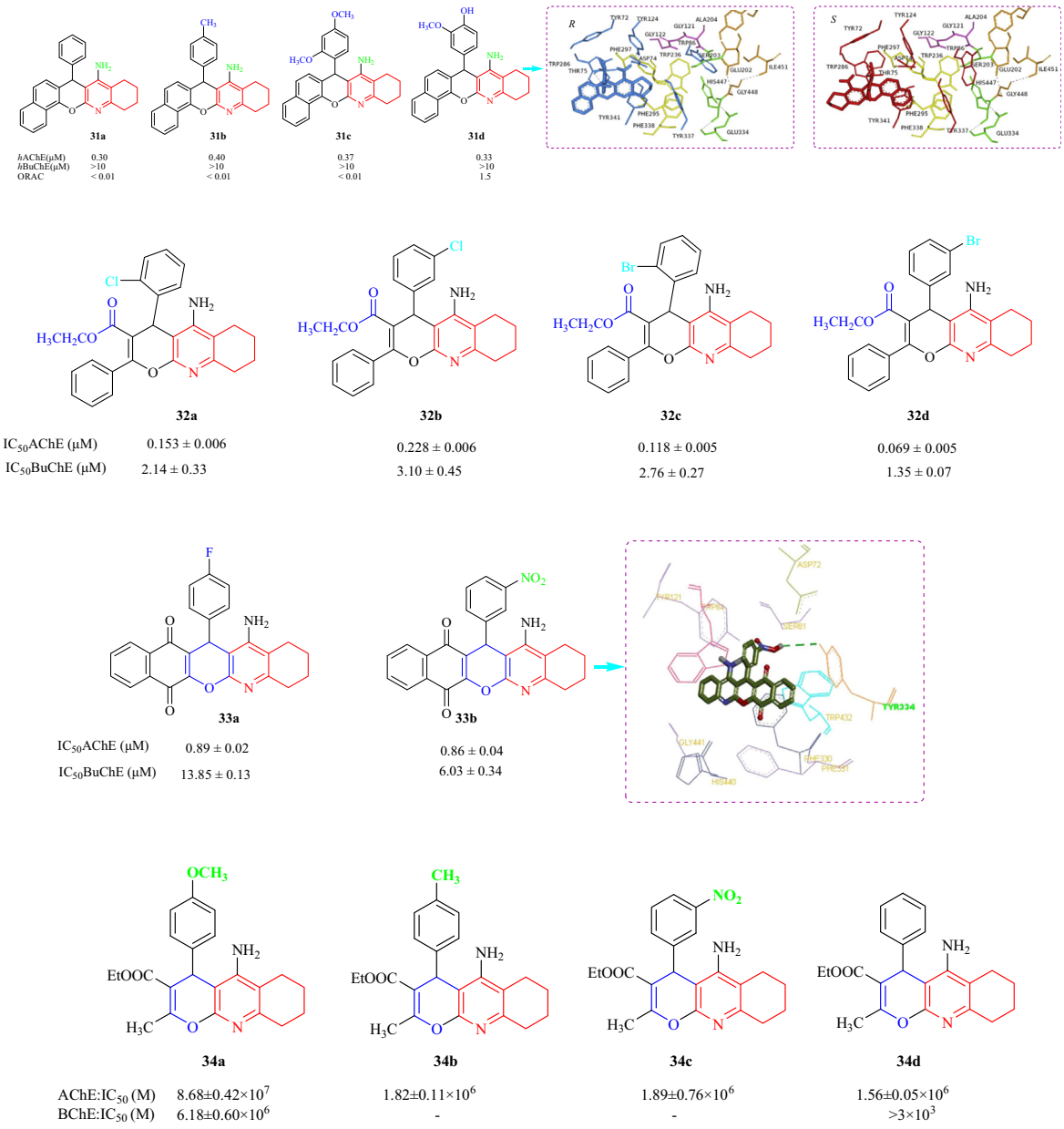

Fig. 10a The structural of tacrine-quinoline and related analogs **31**–**34**.

designed and synthesized a series of multifunctional tacrine derivatives, 4*H*-pyrano[2,3-*b*]quinoline-3-carboxylates (Fig. 10a), as ChE inhibitors. The IC_{50} values against AChE indicated that all the derivatives showed marked inhibitory activity with IC_{50} values from 0.069 to 6.22 μM. The activity increased in the order of 3-Br > 2-Br > 2-Cl > 3-Cl > 2-F > 4-F > 4-NO_2 > 3-F > 4-Cl > 2,4-Cl_2 > 3-NO_2 > 4-Br for the electron-withdrawing groups. The order of the activity was H > 4-OCH_3 > 3-OCH_3 > 4-CH_3 for electron-donating groups. And the study found the electron-withdrawing groups were more effective than electron-donating groups for AChE inhibition. Among the tested compounds, **32d** exhibited the most potent inhibition of AChE and BuChE with IC_{50}values of 0.069 and 1.35 μM of, respectively. Inhibition assays showed that most derivatives exhibited potent activity against AChE and the potential for activity against BuChE. Analysis of the SAR concluded that Cl or Br substituents at the *ortho*- or *meta*- positions of the 4-benzene ring can increase the anti-cholinesterase effects. Mahdavi et al. (Mahdavi, et al., 2019a) have synthesized 17 benzochromeno-quinolinone compounds as tacrine analogs and evaluated the pharmacological action with the aim of developing anti-AD agents (Fig. 10a). Fifteen compounds showed AChE inhibition (IC_{50} = 0.86–27.52 μM). Two analogs **33a** and **33b** were discovered to be good anti-AChE and anti-BChE agents with IC_{50} = 0.86 and 0.89 μM and IC_{50} = 6.03 and 13.85 μM, respectively. Surprisingly, **33b** had an inhibitory effect on β-secretase 1 (IC_{50} = 19.60 μM), as well as the ability to chelate Cu^{2+}, Fe^{2+}, and Zn^{2+}. In addition, the effect of halogenations had no significant effect, but the position of the substituent on the aryl moiety was important for AChE inhibitory activity, the order of activity of 2-halo substituted

compounds was 2-bromine > 2-chlorine > 2-fluorine. In contrast, the order of activity was 4-fluorine > 4-bromine > 4-chlorine. In the molecular docking assay of **33b**, a hydrogen bond was formed between **33b** and Tyr334. In 2001, Marco et al. (Marco et al., 2001) investigated the AChE and BChE inhibitory activity of a family of pyrano[2,3-*b*]quinolones. The tested analogs showed less activity than tacrine (IC_{50} = 1.3 × 10^{-7} M). The most active compound was **34a** with IC_{50} = 8.86 ± 0.42 × 10^{7} M, which was approximately-seven times less active compound (Fig. 10a). Analysis of the SAR of the compounds indicated: (1) the type of substituents on the aromatic ring at C4 appeared to have no effect on the inhibition; (2) the order of AChE inhibitory activity of the substituted derivatives was 4-OCH_3 > H > 4-CH_3 > 3-NO_2 > 4-Cl > 4–CN; (3) electron-donating substituents increased the activity more than electron-withdrawing substituents; and (4) replacing the phenyl ring in tacrine with a pyran ring yielded an analog with better AChE inhibitory activity.

Khoobi et al. (Khoobi, et al., 2015) have designed and prepared a series of 2,4,6,7,8,9-hexahydro- pyrazolo[4′,3′:5,6]pyrano[2,3-*b*]quinolin-5-amine analogs, and evaluated the anticholinesterase activity *in vitro*. The IC_{50} values indicatedthat the synthesized analogs, with the exception of the 2-OCH_3-phenyl substituents, showed AChE inhibition (IC_{50} = 0.19–3.27 μM). The most active analog was compound **35b** with 3,4-diOCH_3-phenyl substituents with an IC_{50} value of 0.19 μM (Fig. 10b), which was more active than tacrine. However, the 4-OCH_3-phenyl and 1-naphthyl compounds were almost as effective against AChE as tacrine. For electron-donating groups, the order of AChE inhibitory activity was 3,4-diOCH_3 > 4-OCH_3 > 2,5-diOCH_3 > 3,4,5-triOCH_3 > 2-OCH_3. The molecular modeling of AChE with **35** *R*- and *S*-enantiomers indicated *R*-enantiomer, dimethoxy-phenyl moiety oriented toward the CAS, 3,4-diOCH_3-phenyl moiety was a *T*-shape π-π stacking with Phe330 and hydrogen binding with His440. *S*- toward PAS, *T*-shape π-π stacking of 3,4-diOCH_3-phenyl with Trp279 and a hydrogen bond between pyrazole ring and Ser286. Pourabdi et al. (Pourabdi et al., 2016) have designed and prepared a class of tacrine-based pyrazolo [4′,3′:5,6]pyrano[2,3-*b*]quinolines derivatives as inhibitors of AChE and BuChE for anti-AD activity. The majority of the derivatives inhibited AChE (IC_{50} < 2 μM), in particular, the 3-propyl compound **36a**, 3-phenyl derivatives **36b** and **36c**, and the 3-(furan-2-yl) analog **36d** showed superior activity compared with tacrine (Fig. 10b). **36c** (IC_{50} = 0.034 μM) was six times more active than tacrine. In addition, all the derivatives inhibited BuChE (IC_{50} values ≤ 0.570 μM), except for the tri-phenyl (R_1 = R_2 = R_3 = Ph) derivative, and most compounds inhibited BuChE to a greater extent than AChE. The putative binding mode of **36c** in the AChE binding site displayed the pyrazole fragment was involved in hydrogen bonding to Glu199, the cyclohexyl moiety was installed in the hydrophobic pocket by Trp84, Phe330, Trp432 and Ile439. The interactions between **36c** and BuChE displayed binding site Ser198 and Trp82 were inclued in binding with ligand through hydrogen bond and *T*-shape π-π interaction, respectively, another hydrogen bonding was exhibted between pyra-

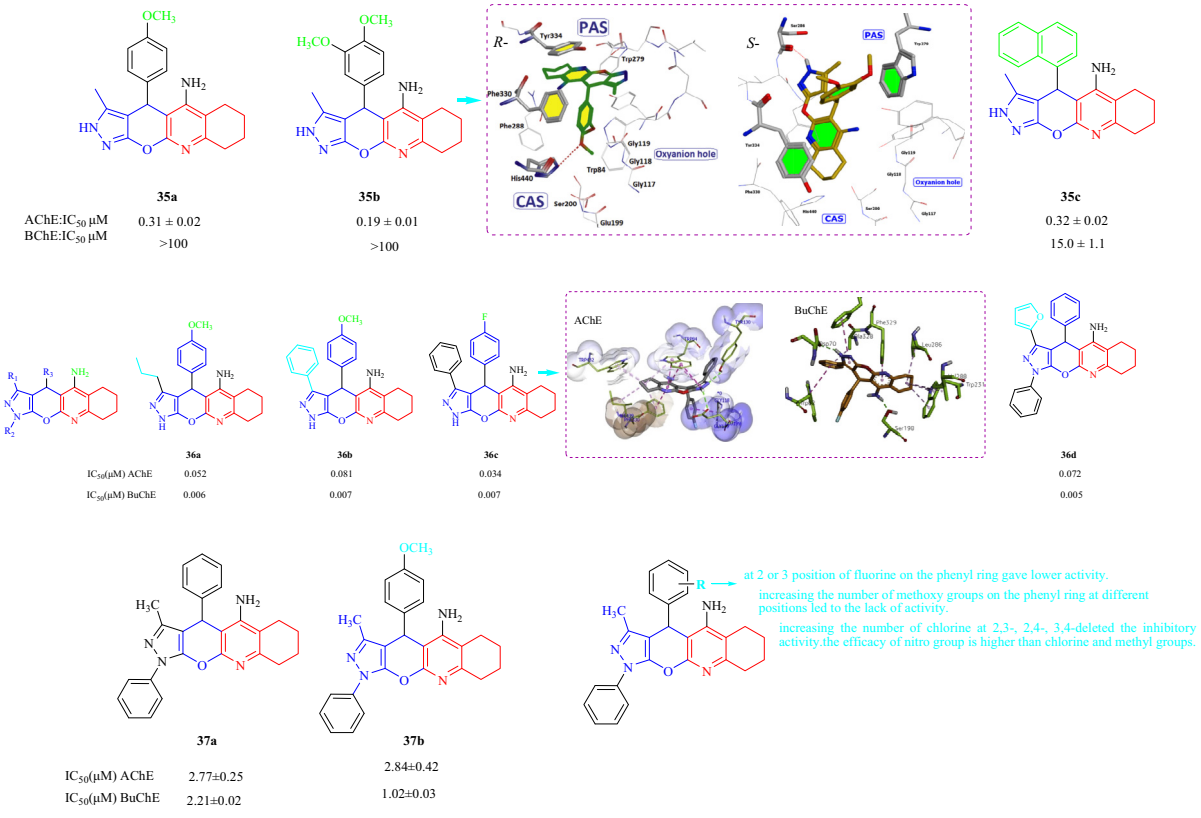

Fig. 10b The anti-Alzheimer of structural tacrine-quinoline and related analogs **35**–**37**.

zole ring and Asp70, aliphatic cyclohexyl fragment is directed into the lipophilic pocket formed by residues Leu286, Val288 and Trp231. In 2017, Mahdavi et al. (Mahdavi, et al., 2017b) prepared a family of pyrazolo[4′,3′:5,6]pyrano [2,3-*b*] quinolin-5-amines, and assessed AChE and BuChE inhibition *in vitro*. Eleven derivatives showed potent AChE inhibition (IC_{50} = 2.77–29.57 μM), compound **37a** with a phenyl substituent at the 4-position displayed the highest inhibitory activity (IC_{50} = 2.77 μM). Eight compounds had good inhibitory activity against BuChE (IC_{50} values from 0.06 to 10.0 μM), and the compound with a 2,4-diOCH_3-phenyl group displayed the best BuChE inhibitory activity (IC_{50} = 0.06 μM). The SAR analysis is shown in Fig. 10b. Overall, derivatives **37a** and **37b** showed good activity against AChE and BChE.

In 2013, Khoobi et al. (Khoobi, et al., 2013) reported a class of 8-amino-tetrahydrochromeno [3′,4′:5,6] pyrano[2, 3-*b*] quinolin-6(7*H*)-one analogs and evaluated the AChE and BuChE inhibition. Most of the prepared derivatives displayed selective activity against AChE and three compounds **38a**, **38b**, and **38c** showed better activity against *ee*AChE with IC_{50} values of 5, 14, and 16 nM, respectively, compared with the other compounds (Fig. 10c). **38a** (with a 4-F-phenyl substituent) displayed the best activity against *ee*AChE. The compounds with methyl, ethyl, and 3-fluorophenyl groups at the 7-positioncan be thought of as dual inhibitors for both enzymes. In the analysis of the SAR of this series of compounds, the order of AChE inhibitory activity was *n*-butyl > ethyl > methyl for alkyl substituents at position 7; the activity for heteroaryl substituents had the following order: benzodioxole-5-yl > 4-pyridyl > 2-thienyl; and the order of activity for the substituents on the phenyl ring at position 7 was 4-F > 2-Cl > 2,4-Cl_2 > 3-F > 4-Cl > 3-NO_2 > 3-Cl for electron-withdrawing groups and 4-CH_3 > 3,4,5-tri-OCH_3 for electron-donating groups. Molecular modeling of AChE with **38a** indicated a hydrogen bonding of coumarin carbonyl moiety with hydroxyl of Tyr121. The phenyl ring at position 7 was oriented toward the hydrophobic pocket of the binding cavity composed of Phe330, Tyr334 and Phe331. Hariri et al. (Hariri, et al., 2016) have designed and synthesized a family of pyrano [3′,4′:5,6] pyrano[2,3-*b*]quinolinone derivatives and assessed the tested compounds for AChE and BChE inhibition *n vitro*. The synthesized compounds exhibited good AChE inhibition with IC_{50} values from 0.37 to 5.62 μM. However, most of the tested derivatives did not display BChE inhibition. Among the tested compounds, compound **39a** with 2,3-dichlorine atoms on the aromatic ring displayed the greatest AChE inhibition (IC_{50} = 0.37 μM) (Fig. 10c). Furthermore, derivatives with 2-NO_2-5-Cl, 2-Cl, and 4-Cl substituents displayed better anti-AChE effects with IC_{50} values of 0.72, 0.80, and 0.82 μM, respectively. The electronic features of the substituents and their positions on the 12-aryl group played important roles in the AChE inhibitory activity. In analysis

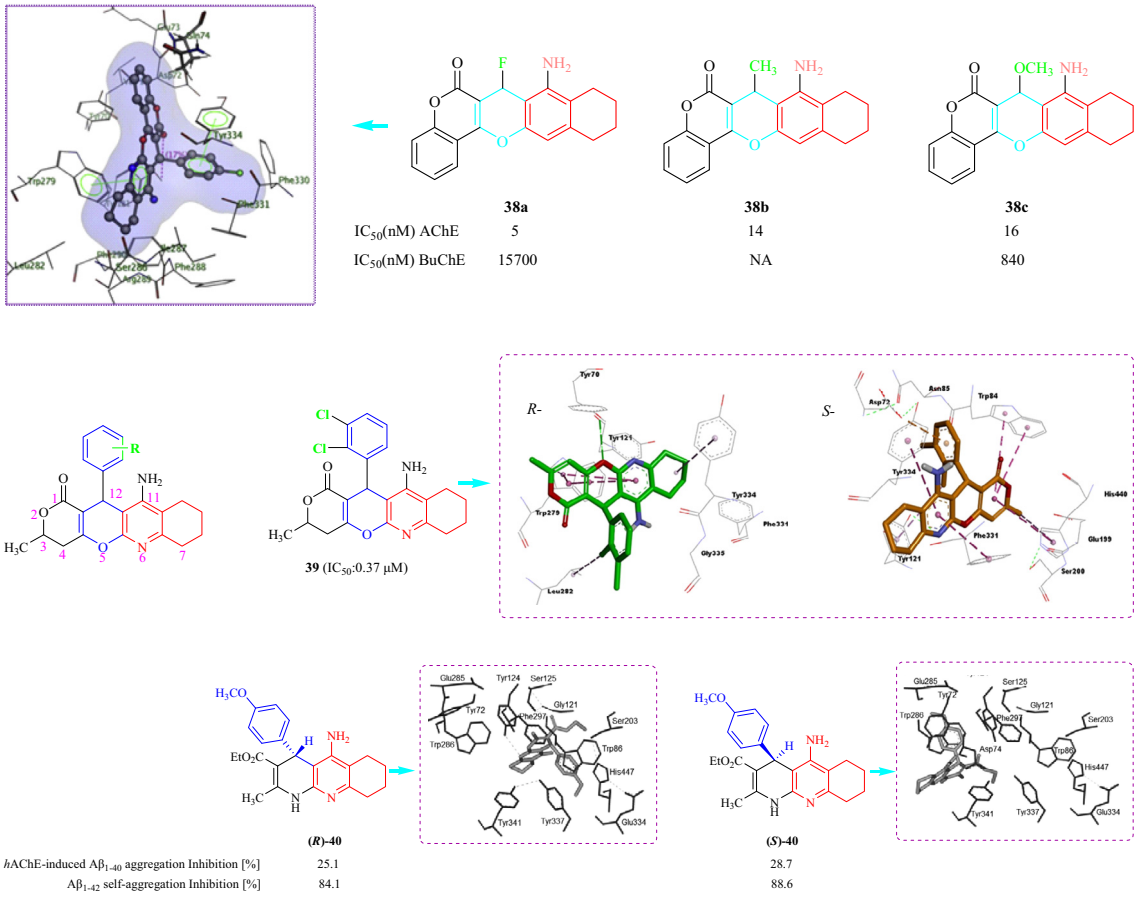

Fig. 10c The anti-Alzheimer of structural tacrine-quinoline and related analogs **38**–**40**.

of the SAR, the order of AChE inhibitory activity for the electron-withdrawing groups was 2,3-diCl > 2-NO_2-5-Cl > 4-Cl > 2-Cl > 2-NO_2 > 3-NO_2 > 2-F > 4-F; and for electron-donating groups was 4-Me > 3-Me > H > 2-Me ≈ 4-Me O > 3,4,5-triMeO. The molecular modeling of AChE with **39** *R*- and *S*-enantiomers indicated *R*-enantiomer 2,3-diCl moiety oriented toward Leu282 and hydrophobic interaction oriented toTyr70, Tyr121, Tyr334,Trp279 residues of PAS, for *S*-enantiomers 2,3-diCl moiety has oriented toward Asp72 of the PAS. In 2011, Bartolini et al. (Bartolini, et al., 2011) reported the synthesis and the evaluation of the AChE inhibition and $A\beta_{1-42}$ self-aggregation *in vitro* of (*R*/*S*)-*p*-methoxytacripyrine (**40**) (Fig. 10c). **40** could have inhibitory activity against both ChEs by modulation of the chirality at the stereocenter C4. Specifically, enantiomer (*S*)-**40** ($A\beta_{1-42}$ self-aggregation inhibition: 88.6 %) had approximately 10-fold greater inhibitory activity than (*R*)-**40** ($A\beta_{1-42}$ self-aggregation inhibition: 84.1 %). Molecular docking simulation AChE with **40** *R*- and *S*-enantiomers suggested *R*-40 *h*AChE placed in the binding pocket residues involved in catalysis, Ser203, Glu334, His447, indole ring of Trp286 forms a π-π interaction with *p*-OCH_3-phenyl ring, a hydrogen bond between amino group of *S*-40 and carboxylate group of Asp74.

In 2017, Chen et al. (Chen, et al., 2017) have prepared a class of tacrine-ferulic acid analogs as multi-target ChE inhibitors and 36 analogs had inhibitory activity against AChE with IC_{50} values < 100 nM. Among two compounds **41a** and **41b** displayed the best inhibitory effects. **41a** exhibited *h*AChE inhibition (IC_{50} = 60.6 ± 5.6 nM), and *h*BuChE inhibition (IC_{50} = 86.1 ± 15.5 nM) and **41b** showed *h*AChE inhibition (IC_{50} = 55.1 ± 4.9 nM) and *h*BuChEI inhibition (IC_{50} = 5 5.9 ± 3.3 nM) (Fig. 10d). The compounds efficiently inhibited human ChEs. The SAR analysis indicated that methoxy and methyl groups increase inhibitory activity on AChE, which was *para*- > *meta*- > *ortho*-. When substituted by Cl, the activity on AChE was *para*- > *meta*- > *ortho*-, different halogen atoms, the activity was –Cl ≈–Br > –F. The molecular docking of *h*AChE with **41a** indicated tetrahydroacridin moiety formed multiple π–π stacking contacts with the aromatic side chains of Trp86 and Tyr124, while for **41b** formed π–π stacking Trp286 and Tyr341. Hepnarova et al. (Hepnarova, et al., 2018) have designed and synthesized 21 tacrine-benzyl quinolone carboxylic acid analogs and evaluated the compounds as inhibitors of *h*AChE and *h*BChE *in vitro*. Three different series were synthesized with different tacrine cores: unsubstituted tacrine; 6-chlorotacrine; and 7-methoxytacrine. The analogs were inhibitors of ChEs. Compounds **42a**, **42b**, and **42c** showed better AChE inhibition with IC_{50} values of 1.53, 0.129, and 0.0419 μM, respectively (Fig. 10d), compared with the other compounds. In addition, all the analogues demonstrated micromolar to nanomolar *h*BChE inhibition. The SAR analysis displayed linker between two basic pharmacophores played a crucial role in contacting both anionic sites, which found the best effect was two or three methylene units tethered hybrids. In addition, the observation can be made between series with descending *h*AChE affinity from 6-OCH_3-tacrine ≥ unsubsituted tacrine ≥ 7-Cl-tacrine, whcih 7-Cl-tacrine was found to be the most active *h*AChE inhibitor. Docking simulations **42c** with *h*AChE suggested 1,4-dihydroquinoline provide favorable stacking to Tyr341, Tyr124 is engaged in anchoring 4-methoxybenzyl moiety (Fig. 10d). In 2018, Zhu et al. (Zhu, et al., 2018b) designed and prepared a family of tacrine-ferulic acid hybrids modified with a benzyl group to investigate ChE inhibitors asmulti-target ligands. All the tested analogues displayed AChE and BuChE inhibition with IC_{50} values from 37 to 284.1 nM, and 52.7 to 256.7 nM, respectively. Among the tested compounds, **43a** (R = 4-Br), **43b** (R = 3,4-diCH_3), and **43c** (R = 4-CF_3) showed the highest activity against AChE (with IC_{50} values of 49.5, 37.0, and 128.6 nM, respectively), and against BuChE (IC_{50} values of 69.4, 101.4, and 52.7 nM, respectively) (Fig. 10d). The SAR analysis displayed dimethyl substitution at benzyloxyl showed to enhance effects against AChE. The electron-withdrawing groups: –CN and-CF_3 showed reduced AChE inhibitory effect while they were favorable for BuChE inhibition. In addition, Docking simulations **43b** with AChE displayed 1,2,3,4-tetrahydroacridin core was located at CAS by a π-π stacking interaction with Trp86, phenyl core of the ferulic acid moiety formed p-p stacking interactions with Trp286 and Tyr341(Fig. 10d). In 2018, Galdeano et al. (Galdeano, et al., 2018) reported the synthesis of polar tacrine derivatives, including 6-chlorotacrine, and huprine Y, and investigated the inhibition of *h*AChE and *h*BChE. All the derivatives showed *h*AChE and *h*BChE inhibitory effects with IC_{50} values from 0.01 to 12 μM, and 0.05 to 22.3 μM, respectively. Compounds **44a**, **44b**, and **44c** displayed the most potent and selective *h*AChE inhibitory effects of all the derivatives, with IC_{50} values of 0.01, 0.06 and 0.20 μM, respectively, and were selective for *h*AChE and *h*BChE inhibition (Fig. 10d). The SAR analysis showed triazole-containing side chain is terminated with a polyphenol-like aromatic ring, resulting compounds are slightly more potent *h*AChE and *h*BChE inhibitors than the parent tacrine and 6-chlorotacrine. Docking simulations **44a** with *h*AChE indicated triazole ring is engaged in two perpendicular π-stacking interactions with Tyr334, Phe300, and in H-bonds with Tyr121 and Asp72. While **44b** showed huprine plane was shifted away from catalytic His440, and upwards towards Phe330. Hamulakova et al. (Hamulakova, et al., 2021) have prepared two classes of tacrine-indole ligands and evaluated the *h*AChE and *h*BChE inhibitory effects. The tested derivatives showed *h*ChE inhibitory activity with IC_{50} values from 160 to 25 nM and 160 to 39 nM for *h*AChE and *h*BChE, respectively. Compounds **45a** and **45b** showed the best inhibition for AChE with IC_{50} values of 25 and 70 nM, respectively (Fig. 10d). The analysis of the SAR suggested four-methylene spacer appeared to best *h*AChE inhibition, six-methylene bridge conferred the best inhibition to *h*BChE, methoxy group on indole nitrogen enhanced inhibitory activity for *h*BChE with a chain length of n = 4–6. In 2022, the Przybyłowska group designed and synthesized a family of 14 *N*- and *O*-phosphorylatedtacrine analogs and investigated the inhibitory effects against *h*AChE and *h*BChE as latent anti-AD agents (Przybyłowska, et al., 2022). The tested analogs displayed activity against AChE with IC_{50} values from 6.11 to 676.7 nM, respectively, and against BuChE (IC_{50} = 1.969–186.2 nM). The compounds with the most inhibitory activity against AChE were **46a** (pIC_{50} = 1.513 nM) and **46b** (pIC_{50} = 0.786 nM); and **46c** and **46d** exhibited the best inhibition against BuChE with pIC_{50} values of 0.913and 0.998 nM, respectively. These synthesized compounds also inhibited BChE. In addition, the molecular docking of **46b** was investigated and **46b** exhibited low docking energies of –12.5 and –10.7 kcal/mol for AChE and BChE, respectively.

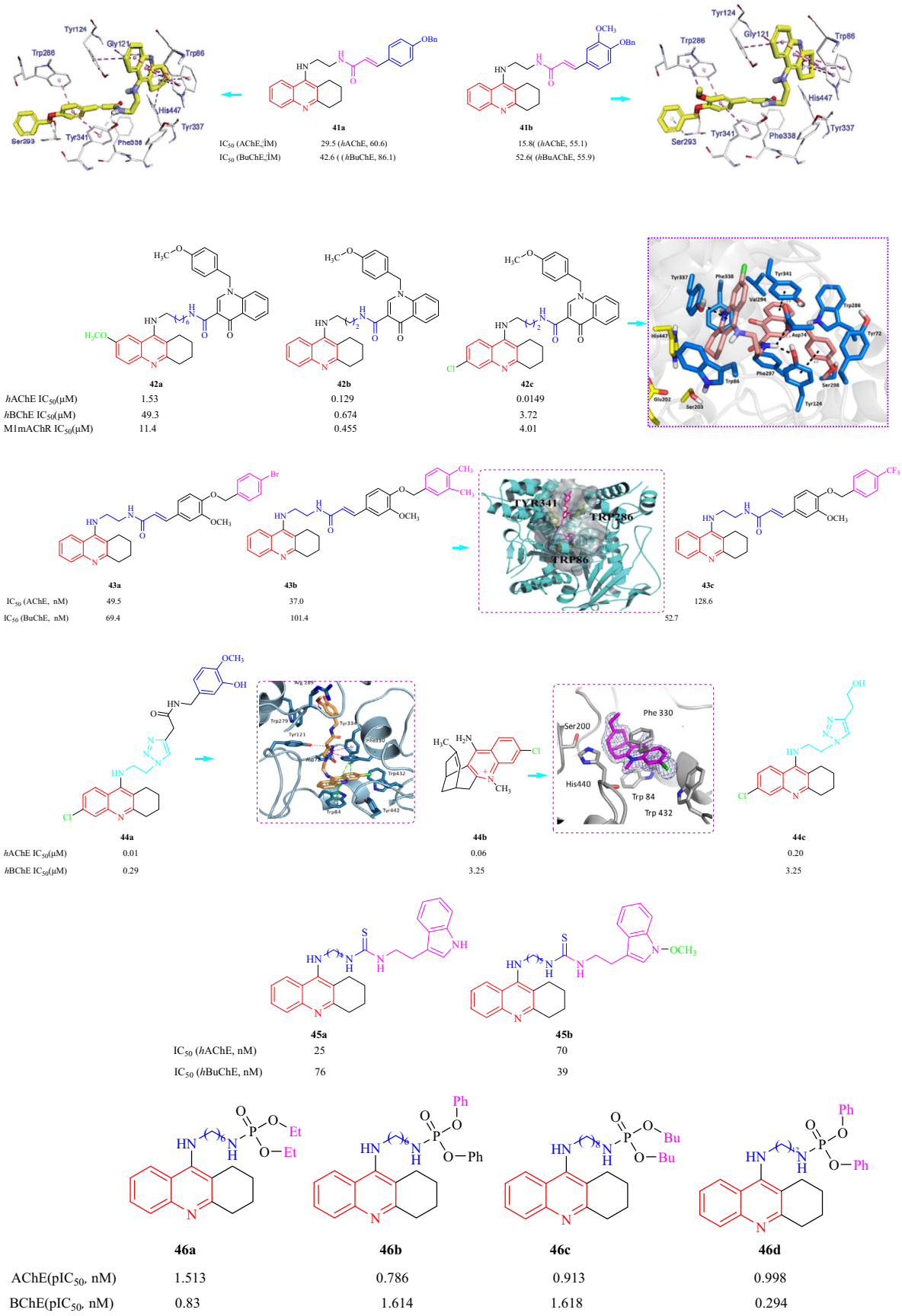

Fig. 10d Structural formula tacrine-quinoline analogs **41**–**46.**

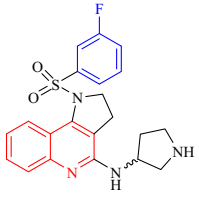

47a **47b**

5-HT$_6$ (K_i [nM])	(*S*):7; (*R*):12	(*S*):3; (*R*):7
5-HT$_6$ (K_b[nM])	(*S*):0.83; (*R*):12	(*S*):0.41; (*R*):6.1

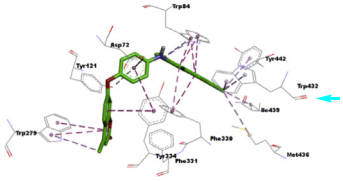

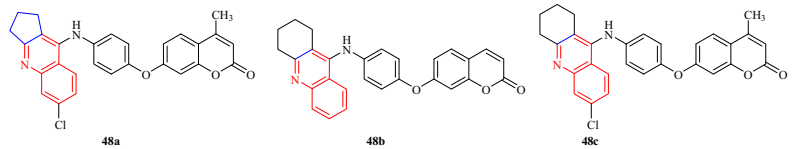

48a **48b** **48c**

AChE inhibition [IC_{50} μM]	16.17	19.07	18.03
BuChE inhibition [IC_{50} μM]	> 100	28.67	31.20

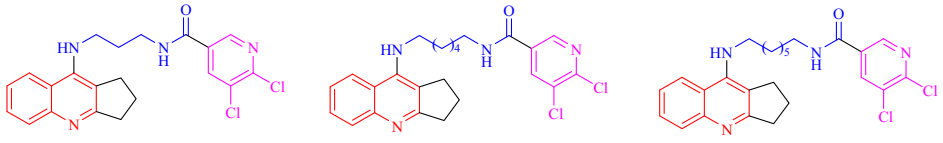

49a **49b** **49c**

AChE inhibition [IC_{50} μM]	0.052	0.053	0.125
BuChE inhibition [IC_{50} μM]	0.158	0.127	0.071

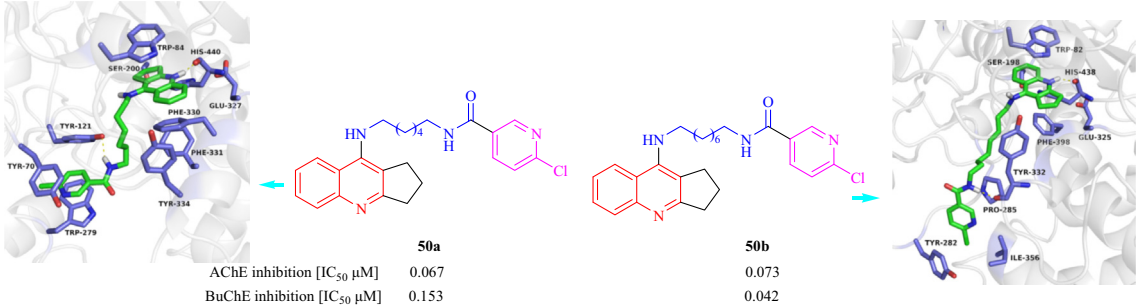

50a **50b**

AChE inhibition [IC_{50} μM]	0.067	0.073
BuChE inhibition [IC_{50} μM]	0.153	0.042

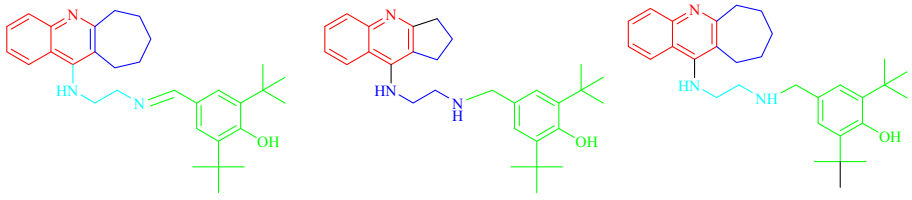

51a **51b** **51c**

*h*AChE, IC_{50} (μM)	4.03	3.50	1.90
*h*BuChE, IC_{50} (μM)	0.419	0.652	0.084

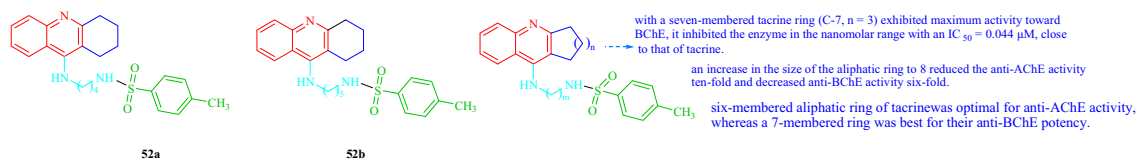

52a **52b**

*h*AChE, IC_{50} (μM)	0.668	0.131
*h*BuChE, IC_{50} (μM)	0.0617	0.068

Fig. 11a Structural formula tacrine-quinoline and related analogs **47**–**52**.

In 2016, Grychowska et al. (Grychowska, et al., 2016) have also reported a class of arylsulfonyl analogues based on *N*-4-(pyrrolidin-3-yl-amino)-1*H*-pyrrolo[3,2-*c*]quinoline as 5-HT_{6R} antagonists. The 18 synthesized compounds showed medium to high affinity for the 5-HT_{6R} with K_i values from 3 to 101 nM. Among them, compounds **47a** and **47b** exhibited the most affinity for the 5-HT_{6R} [with K_i values of 7 ± 1 (*S*-enantiomer) and 12 ± 3 (*R*-enantiomer) and 3 ± 1 (*S*-enantiomer) and 7 ± 2 (*R*-enantiomer), respectively] (Fig. 11a). However, it was suggested that the *S* isomers were the best antagonists and displayed a better antagonistic action on the 5-HT_6 sites. The SAR analysis suggested *tert*-butyl or isopropyl groups in *para* position significantly decreased affinity, suggesting that bulky substituents at this position were unfavorable for binding to the 5-HT_{6R}. The electron-withdrawing substituent in *meta* position of phenyl ring with electron-donating methoxy or methyl groups maintained the high affinity for 5-HT_{6R}. Najafi et al. (Najafi, et al., 2016) have designed and synthesized a family of acridine-chromenone and quinoline-chromenone derivatives and assessed the AChE and BuChE inhibition. Twelve compounds displayed anti-AChE effects (IC_{50} = 16.17–83.10 μM). Most of the analogs did not show any effects against BChE. Among the tested compounds, **48a** with CH_3 and Cl substituents displayed the best inhibitory activity (IC_{50} = 16.17 μM). Substitution of the five-membered ring (in **48a**) with a 6-membered ring, resulted in the formation of a tetrahydroacridine scaffold (**48b**), which decreased the inhibitory activity against AChE (IC_{50} = 18.03 μM). **48c** with a tetrahydroacridine moiety and no other substituents had an IC_{50} value of 19.07 μM. The SAR analysis displayed five or six-membered ring induce more activity, seven-membered ring fused to quinoline moiety which showed lower activity comparing with its counterpart. Docking simulations **48a** with *h*AChE showed π-π interactions between quinoline moiety and Trp84 and Phe330, hydrophobic interaction of Cl with Ile439, Met436, Tyr442 and Trp432, phenoxy group occupied to make π-anion interaction with Asp72 and π-π interaction with Phe330, 4-methylchromenone moiety established π-π and hydrophobic interaction with Trp279 (Fig. 11a). Czarnecka et al. (Czarnecka, et al., 2017a) have reported a series of 2,3-dihydro-1*H*-cyclopenta[*b*]quinoline derivatives using 5,6-dichloronicotinic acid. All the synthesized derivatives were AChE inhibitors with IC_{50} values ranging from 0.052 to 0.744 μM. Among the reported derivatives, **49a** (IC_{50} = 0.052 μM) and **49b** (IC_{50} = 0.053 μM) showed greater inhibition of AChE, which was three and two times that of tacrine and donepezil, respectively. All the derivatives also showed good BuChE inhibitionwithIC_{50} values ranging from 0.071 to 1.863 μM. The most active compound toward BuChE, **49c**, had an IC_{50} value of 0.071 μM (Fig. 11a). In addition, in 2019, Czarnecka et al. (Czarnecka et al., 2019b) reported eight cyclopentaquinoline derivatives with a tetrahydroacridine structure and evaluated the *Ee*AChE and *Eq*BuChE inhibition *in vitro*. Four compounds exhibited IC_{50} values below 100 nM for *Ee*AChE inhibition, which suggested the best inhibition was obtained with alkyl linkers with 6 to 9 carbons in the chain. Eight compounds also displayed inhibitory activity against BuChE with IC_{50} values ranging from 42 to 662 nM. Among these compounds, compounds **50a** and **50b** displayed the most activity against *Ee*AChE and *Eq*BuChE with IC_{50} values of 0.067 and 0.073 μM, respectively and 0.153 and 0.042 μM, respectively. The molecular docking of *h*AChE with **50a** indicated an amide nitrogen atom formed a hydrogen bond with hydroxyl group of Tyr121 toward AChE. While for 50b with BuChE, a hydrogen bond was with the main chain of Tyr332 in anionic site (Fig. 11a). Makhaeva et al. (Makhaeva, et al., 2020a) have reported the synthesis of two series of derivatives of 4-amino-2,3-polymethylenequinoline. All the derivatives inhibited AChE and BChE, displaying selectivity toward BChE (IC_{50} = 0.084–4.27 μM), and with IC_{50} values ranging from 1.90 to 45.0 μM against AChE. Among these compounds, **51a**, **51b**, and **51c** displayed better inhibition of *h*AChE and *h*BuChE with IC_{50} values of 4.03, 3.50 and 1.90 μM, respectively; and 0.419, 0.652 and 0.084 μM, respectively (Fig. 11a). Analysis of the SAR showed to increase of an aliphatic ring size of 4-amino-2,3-polymethylenequinoline fragment from C-5 to C-7 had no effect on anti-AChE activity, whereas its increase to C-8 reduced potency of

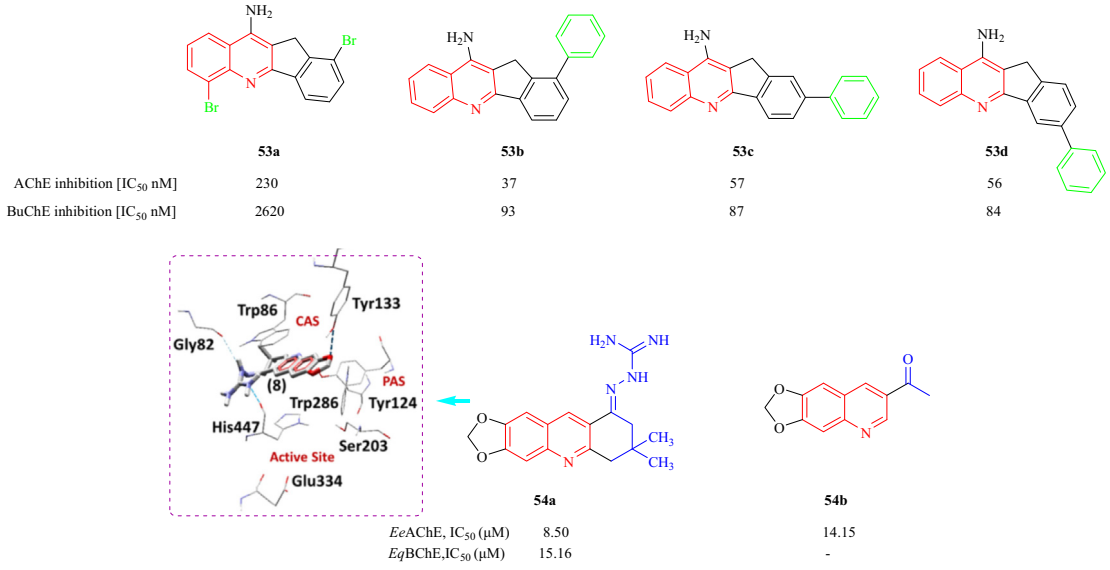

Fig. 11b Structural formula tacrine-quinoline and related analogs **53, 54**.

AChE inhibition ten times, with a cycloheptaquinoline moiety (C-7) exhibited maximum activity toward BChE. In 2020, Makhaeva et al. (Makhaeva, et al., 2020b) also synthesized 11 derivatives of 4-amino-2,3-polymethyl-enequinoline and investigated the ChE inhibition. The tested derivatives displayed inhibitory effects toward AChE (with IC_{50} values from 0.131 to 9.01 μM) and BChE (IC_{50} values from 0.0431 to 0.924 μM), but showed selectivity toward BChE. The SAR results are shown in Fig. 11a. In 2018, Ekiz et al. (Ekiz, et al., 2018) reported the synthesis of bromoindenoquinolines and phenyl-substituted indenoquinoline amine analogs and investigated the inhibition of AChE and BChE (Fig. 11a). The monophenyl indenoquinolines inhibited AChE and BChE with IC_{50}values ranging from 37 to 57 nM and 84 to 93 nM, respectively. Compounds **53a**, **53b**, **53c**, and **53d** displayed good inhibitory effects against AChE with IC_{50} values of 230, 37, 57, and 56 nM, respectively, and against BuChE with IC_{50} values of 2620, 93, 87 and 87 nM, respectively. The SAR analysis displayed the introduction of phenyl substituent on compounds led to increased inhibition effects against AChE and BChE. Six quinoline-piperonal analogs were prepared and the inhibitory activity against AChE and BChE was assessed by De Brum et al. (DeBrum et al., 2019). Five compounds showed *Ee*AChE inhibition with IC_{50} values from 8.50 to 62.76 μM. Compound **54a** showed selectivity for *Ee*AChE over *Eq*BChE; the inhibitory effect on *Ee*AChE (IC_{50} = 8.50 ± 0.39 μM) was twice that of *Eq*BChE (IC_{50} = 15.16 ± 0.75 μM). The docking studies of *Ee*AChE with **54a** indicated the lowest intermolecular energy and the residues Tyr124, Tyr133 and His447 (Fig. 11b).

3. Conclusions

In summary, because the basic properties and extra-binding capacity of the quinoline scaffold play an important role in optimization the physicochemical properties in the drug design and development strategies. Therefore, in recent years, researchers have synthesized hybrid quinoline scaffolds with compounds containing other heterocyclic and evaluated various biological activities, also involving the inhibitory effects against anti-AD effects. The main part of this review focus on and highlights the synthesized quinolone and related analogs, including various heterocyclic such as indole, tacrine, triazole, pyrrolo, chromeno, and pyrano etc as anti-Alzheimer's disease agents from 2001 to 2022, and also particularly highlight the structure–activity relationships and the molecular binding modes. Thus, to find the new characteristic structures or groups, discover the active lead compounds, further design of rationally anti-Alzheimer's disease agents and drug molecules provide the basis.

Acknowledgements

This research was supported by the Province of Jilin Science and Technology Development Plan (No. 20210204115YY), and the Department of Education of Jilin Province (No. JJKH202111444KJ). We thanks Victoria Muir, PhD, from Liwen Bianji, (Edanz) (www.liwenbianji.cn/), edited the English text of a draft of this manuscript.

References

Adlard, P.A., Cherny, R.A., Finkelstein, D.I., Gautier, E., Robb, E., Cortes, M., Volitakis, I., Liu, X., Smith, J.P., Perez, K., Laughton, K., Li, Q.X., Charman, S.A., Nicolazzo, J.A., Wilkins, S., Deleva, K., Lynch, T., Kok, G., Ritchie, C.W., Tanzi, R.E., Cappai, R., Masters, C.L., Barnham, K.J., Bush, A.I., 2008. Rapid restoration of cognition in Alzheimer's transgenic mice with 8-hydroxy quinoline analogs is associated with decreased interstitial Aβ. Neuron 59, 43–55. https://doi.org/10.1016/j.neuron.2008.06.018.

Anand, R., Gill, K.D., Mahdi, A.A., 2014. Therapeutics of Alzheimer's disease: past, present and future. Neuropharmacol. 76, 27–50. https://doi.org/10.1016/j.neuropharm.2013.07.004.

Baccile, J.A., Spraker, J.E., Le, H.H., Brandenburger, E., Gomez, C., Bok, J.W., Macheleidt, J., Brakhage, A.A., Hoffmeister, D., Keller, N.P., Schroeder, F.C., 2016. Plant-like biosynthesis of isoquinoline alkaloids in Aspergillus fumigatus. Nat. Chem. Biol. 12, 419–424. https://doi.org/10.1038/nchembio.2061.

Bartolini, M., Pistolozzi, M., Andrisano, V., Egea, J., López, M.G., Iriepa, I., Moraleda, I., Glvez, E., Marco-Contelles, J., Samadi, A., 2011. Chemical and pharmacological studies on enantiomerically pure p-methoxy- tacripyrines, promising multi-target-directed ligands for the treatment of Alzheimer's disease. ChemMedChem 6, 1990–1997. https://doi.org/10.1002/cmdc.201100239.

Bi, Y., Stoy, P., Adam, L., He, B., Krupinski, J., Normandin, D., Pongrac, R., Seliger, L., Watson, A., Macor, J.E., 2004. Quinolines as extremely potent and selective PDE5 inhibitors as potential agents for treatment of erectile dysfunction. Bioorg. Med. Chem. Lett. 14, 1577–1580. https://doi.org/10.1016/j.bmcl.2003.12.090.

Bondi, M.W., Edmonds, E.C., Salmon, D.P., 2017. Alzheimer's disease: Past, present, and future. J. Int. Neuropsychol. Soc. 23, 818–831. https://doi.org/10.1017/S135561771700100X.

Bosak, A., Opsenica, D.M., Šinko, G., Zlatar, M., Kovarik, Z., 2019. Structural aspects of 4-aminoquinolines as reversible inhibitors of human acetylcholinesterase and butyrylcholine-sterase. Chem. Biol. Interact. 308, 101–109. https://doi.org/10.1016/j.cbi.2019.05.024.

Boyd, D.R., Sharma, N.D., Loke, P.L., Malone, J.F., McRoberts, W. C., Hamilton, J.T.G., 2007. Synthesis, structure and stereochemistry of quinoline alkaloids from Choisya ternata. Org. Biomol. Chem. 5, 2983–2991. https://doi.org/10.1039/b707576f.

Chen, Y., Lin, H.Z., Zhu, J., Gu, K., Li, Q., He, S.Y., Lu, X., Tan, R. X., Pei, Y.Q., Wu, L., Bian, Y.Y., Sun, H.P., 2017. Design, synthesis, in vitro and in vivo evaluation of tacrine-cinnamic acid hybrids as multi-target acetyl-and butyrylcholinesterase inhibitors against Alzheimer's disease. RSC Adv. 7, 33851–33867. https://doi.org/10.1039/c7ra04385f.

Cherny, R.A., Atwood, C.S., Xilinas, M.E., Gray, D.N., Jones, W.D., McLean, C.A., Barnham, K.J., Volitakis, I., Fraser, F.W., Kim, Y. S., Huang, X., Goldstein, L.E., Moir, R.D., Lim, J.T., Beyreuther, K., Zheng, H., Tanzi, R.E., Masters, C.L., Bush, A.I., 2001. Treatment with a copper-zinc chelator markedly and rapidly inhibits β-amyloid accumulation in Alzheimer's disease transgenic mice. Neuron 30, 665–676. https://doi.org/10.1016/s0896-6273(01)00317-8.

Chu, X.M., Wang, C., Liu, W., Liang, L.L., Gong, K.K., Zhao, C.Y., Sun, K.L., 2019. Quinoline and quinolone dimers and their biological activities: An overview. Eur. J. Med. Chem. 161, 101–117. https://doi.org/10.1016/j.ejmech.2018.10.035.

Corio, A., Gravier-Pelletier, C., Busca, P., 2021. Regioselective functionalization ofquinolines through C-Hactivation: A comprehensive review. Molecules 26, 5467. https://doi.org/10.3390/molecules26185467.

Czarnecka, K., Girek, M., Kręcisz, P., Skibiński, R., Łatka, K., Jończyk, J., Bajda, M., Kabziński, J., Majsterek, I., Szymczyk, P., Szymański, P., 2019b. Discovery of new cyclopentaquinoline analogues as multifunctional agents for the treatment of Alzheimer's disease. Int. J. Mol. Sci. 20, 498–520. https://doi.org/10.3390/ijms20030498.

Czarnecka, K., Girek, M., Maciejewska, K., Skibiński, R., Jończyk, J., Bajda, M., Kabziński, J., Sołowiej, P., Majsterek, I., Szymański, P., 2017a. New cyclopentaquinoline hybrids with multifunctional capacities for the treatment of Alzheimer's disease. J. Enzyme

Inhib. Med. Chem. 33, 158–170. https://doi.org/10.1080/14756366.2017.1406485.

DeBrum, J.O.C., Neto, D.C.F., De Almeida, J.S.F.D., Lima, J.A., Kuca, K., França, T.C.C., 2019. Synthesis of new quinoline-piperonal hybrids as potential drugs against Alzheimer's disease. Int. J. Mol. Sci. 20, 3944–3959. https://doi.org/10.3390/ijms20163944.

De-Paula, V.J., Radanovic, M., Diniz, B.S., Forlenza, O.V., 2012. Alzheimer's disease. Subcell Biochem. 65, 329–352. https://doi.org/10.1007/978-94-007-5416-4_14.

Di Mola, A., Tedesco, C., Massa, A., 2019. Metal-Free air oxidation in a convenient cascade approach for the access toisoquinoline-1,3,4 (2H)-triones. Molecules 24, 2177. https://doi.org/10.3390/molecules24112177.

Eghtedari, M., Sarrafi, Y., Nadri, H., Mahdavi, M., Moradi, A., Homayouni Moghadam, F., Emami, S., Firoozpour, L., Asadipour, A., Sabzevari, O., Foroumadi, A., 2017. New tacrine-derived AChE/BuChE inhibitors: synthesis and biological evaluation of 5-amino-2-phenyl-4H-pyrano[2,3-b]quinoline-3-carboxylates. Eur. J. Med. Chem. 128, 237–246. https://doi.org/10.1016/j.ejmech.2017.01.042.

Ekiz, M., Tutar, A., Ökten, S., Bütün, B., Koçyiğit, Ü.M., Taslimi, P., Topçu, G., 2018. Synthesis, characterization, and SAR of arylated indenoquinoline-based cholinesterase and carbonic anhydrase inhibitors. Arch. Pharm. Chem. Life Sci. 351, e1800167.

Fabiano-Tixier, A.S., Elomri, A., Blanckaert, A., Seguin, E., Petitcolas, E., Chemat, F., 2011. Rapid and green analytical method for the determination ofquinolinealkaloids fromCinchona succirubrabased on microwave-integrated extraction and leaching (MIEL) prior to high performance liquid chromatography. Int. J. Mol. Sci. 12, 7846–7860. https://doi.org/10.3390/ijms12117846.

Farina, R., Pisani, L., Catto, M., Nicolotti, O., Gadaleta, D., Denora, N., Soto-Otero, R., Mendez-Alvarez, E., Passos, C.S., Muncipinto, G., Altomare, C.D., Nurisso, A., Carrupt, P.A., Carotti, A., 2015. Structure-based des-ign and optimization of multitarget-directed 2H-chromen-2-one derivatives as potent inhibitors of monoamine oxidase B and cholinesterases. J. Med. Chem. 58, 5561–5578. https://doi.org/10.1021/acs.jmedchem.5b00599.

Felicetti, T., Mangiaterra, G., Cannalire, R., Cedraro, N., Pietrella, D., Astolfi, A., Massari, S., Tabarrini, O., Manfroni, G., Barreca, M.L., Cecchetti, V., Biavasco, F., Sabatini, S., 2020. C-2 phenyl replacements to obtain potentquinoline-basedStaphylococcus aureus Nor A inhibitors. J. Enzyme Inhib. Med. Chem. 35, 584–597. https://doi.org/10.1080/14756366.2020.1719083.

Fernández-Bachiller, M.I., Pérez, C., González-Muñoz, G.C., Conde, S., López, M.G., Villarroya, M., García, A.G., Rodríguez-Franco, M.I., 2010. Novel tacrine-8-hydroxyquinoline hybrids as multifunctional agents for the treatment of Alzheimers disease, with neuroprotective, cholinergic, antioxidant, and copper-complexing properties. J. Med. Chem. 53, 4927–4937. https://doi.org/10.1021/jm100329q.

Fiorito, J., Saeed, F., Zhang, H., Staniszewski, A., Feng, Y., Francis, Y.I., Rao, S., Thakkar, D.M., Deng, S.X., Landry, D.W., Arancio, O., 2013. Synthesis of quinoline derivatives: Discovery of a potent and selective phosphodies terase 5 inhibitor for the treatment of Alzheimer's disease. Eur. J. Med. Chem. 60, 285–294. https://doi.org/10.1016/j.ejmech.2012.12.009.

Fu, J., Bao, F.Q., Gu, M., Liu, J., Zhang, Z.P., Ding, J.L., Xie, S.S., Ding, J.S., 2020. Design, synthesis and evaluation of quinolinone derivatives containing dithiocarbamate moiety as multifunctional AChE inhibitors for the treatment of Alzheimer's disease. J. Enzyme. Inhib. Med. Chem. 35, 118–128. https://doi.org/10.1080/14756366.2019.1687460.

Gal, S., Zheng, H., Fridkin, M., Youdim, M.B., 2005. Novel multifunctional neuroprotective iron chelator-monoamine oxidase inhibitor drugs for neurodegenerative diseases. selective brain monoamine oxidase inhibition and prevention of MPTP-induced striatal dopamine depletion. J. Neurochem. 95, 79–88. https://doi.org/10.1111/j.1471-4159.2005.03341.x.

Galdeano, C., Coquelle, N., Cieslikiewicz-Bouet, M., Bartolini, M., Pérez, B., Victòria Clos, M., Silman, I., Jean, L., Colletier, J.P., Renard, P.Y., Muñoz-Torrero, D., 2018. Increasing polarity in tacrine and huprine derivatives: potent anticholinesterase agents for the treatment of myasthenia gravis. Molecules 23, 634. https://doi.org/10.3390/molecules23030634.

Gerring, Z.F., Gamazon, E.R., White, A., Derks, E.M., 2021. Integrative network-based analysis reveals gene networks and novel drug repositioning candidates for Alzheimer disease. Neurol. Genet. 7, e622.

Grychowska, K., Satała, G., Kos, T., Partyka, A., Colacino, E., Chaumont-Dubel, S., Bantreil, X., Wesołowska, A., Pawłowski, M., Martinez, J., Marin, P., Subra, G., Bojarski, A.J., Lamaty, F., Popik, P., Zajdel, P., 2016. Novel 1*H*-pyrrolo[3,2-*c*]quinoline based 5-HT6 receptor antagonists with potential application for the treatment of cognitive disorders associated with Alzheimer's disease. ACS Chem. Neurosci. 7, 972–983. https://doi.org/10.1021/acschemneuro.6b00090.

Hampel, H., Mesulam, M.M., Cuello, A.C., Farlow, M.R., Giacobini, E., Grossberg, G.T., Khachaturian, A.S., Vergallo, A., Cavedo, E., Snyder, P.J., Khachaturian, Z.S., 2018. The cholinergic system in the pathophysiology and treatment of Alzheimer's disease. Brain 141, 1917–1933. https://doi.org/10.1093/brain/awy132.

Hamulakova, S., Kudlickova, Z., Janovec, L., Mezencev, R., Deckner, Z.J., Chernoff, Y.O., Janockova, J., Ihnatova, V., Bzonek, P., Novakova, N., Hepnarova, V., Hrabinova, M., Jun, D., Korabecny, J., Soukup, O., Kuca, K., 2021. Design and synthesis of novel tacrine–indole hybrids as potential multitarget-directed ligands for the treatment ofAlzheimer's disease. Future Med. Chem. 13, 785–804. https://doi.org/10.4155/fmc-2020-0184.

Hariri, R., Afshar, Z., Mahdavi, M., Safavi, M., Saeedi, M., Najafi, Z., Sabourian, R., Karimpour-Razkenari, E., Edraki, N., Moghadam, F.H., Shafiee, A., Khanavi, M., Akbarzadeh, T., 2016. Novel tacrine-based pyrano[3′,4′:5,6]pyrano[2,3-*b*]quinolinones: synthesis and cholinesterase inhibitory activity. Arch. Pharm. Chem. Life Sci. 349, 1–10. https://doi.org/10.1002/ardp.201600123.

He, Q.D., Huang, G., Chen, Y.X., Wang, X.Q., Huang, Z.S., Chen, Z. G., 2017. The protection of novel 2-arylethenylquinoline derivatives against impairment of associative learning memory induced by neural Aβ in C. elegans Alzheimer's disease model. Neurochem. Res. 42, 3061–3072. https://doi.org/10.1007/s11064-017-2339-0.

Hepnarova, V., Korabecny, J., Matouskova, L., Jost, P., Muckova, L., Hrabinova, M., Vykoukalova, N., Kerhartova, M., Kucera, T., Dolezal, R., Nepovimova, E., Spilovska, K., Mezeiova, E., Pham, N.L., Jun, D., Staud, F., Kaping, D., Kuca, K., Soukup, O., 2018. The concept of hybrid molecules of tacrine and benzyl quinolone carboxylic acid (BQCA) as multifunctional agents for Alzheimer's disease. Eur. J Med. Chem. 150, 292–306. https://doi.org/10.1016/j.ejmech.2018.02.083.

Iqbal, K., Grundke-Iqbal, I., 2000. Alzheimer disease is multifactorial and heterogeneous. Neurobiol. Agin. 21, 901–902. https://doi.org/10.1016/s0197-4580(00)00191-3.

Jakob-Roetne, R., Jacobsen, H., 2009. Alzheimer's disease: from pathology to therapeutic approaches. Angew. Chem. Int. Ed Engl. 48, 3030–3059. https://doi.org/10.1002/anie.200802808.

Kankanala, J., Marchand, C., Abdelmalak, M., Aihara, H., Pommier, Y., Wang, Z.Q., 2016. Isoquinoline-1,3-diones as selective inhibitors of tyrosyl DNA phosphodiesterase II (TDP2). J. Med. Chem. 59, 2734–2746. https://doi.org/10.1021/acs.jmedchem.5b01973.

Kaur, R., Kumar, K., 2021. Synthetic and medicinal perspective ofquinolinesas antiviral agents. Eur. J. Med. Chem. 215,. https://doi.org/10.1016/j.ejmech.2021.113220 113220.

Khoobi, M., Alipour, M., Moradi, A., Sakhteman, A., Nadri, H., Razavi, S.F., Ghandi, M., Foroumadi, A., Shafiee, A., 2013. Design, synthesis, docking study and biological evaluation of some novel tetrahydrochromeno[3′,4′:5,6]pyrano[2,3-*b*]quinolin-6(7*H*)-

one derivatives against acetyl- and butyrylcholinesterase. Eur. J. Med. Chem. 68, 291–300. https://doi.org/10.1016/j.ejmech.2013.07.045.

Khoobi, M., Ghanoni, F., Nadri, H., Moradi, A., Hamedani, M.P., Moghadam, F.H., Emami, S., Vosooghi, M., Zadmard, R., Foroumadi, A., Shafiee, A., 2015. New tetracyclic tacrine analogs containing pyrano[2,3-*c*]pyrazole:efficient synthesis, biological assessment and docking simulation study. Eur. J. Med. Chem. 89, 296–303. https://doi.org/10.1016/j.ejmech.2014.10.049.

Kim, J.P., Kim, B.H., Bice, P.J., Seo, S.W., Bennett, D.A., Saykin, A. J., 2021. Correction to: BMI1 is associated with CSF amyloid-β and rates of cognitive declinein Alzheimer's disease. Alzheimers Res. Ther. 13, 164. https://doi.org/10.1186/s13195-022-00960-6.

Kim, K.W., Lee, S.Y., Choi, J., Chin, J., Lee, B.H., Na, D.L., Choi, J. H., 2020. A comprehensive evaluation of the process of copying a complex figure in early- and late-onsetAlzheimer disease: a quantitative analysis of digital pen data. J. Med. Internet. Res. 22, e18136.

Knez, D., Brus, B., Coquelle, N., Sosič, I., Šink, R., Brazzolotto, X., Mravljak, J., Colletier, J.P., Gobec, S., 2015. Structure-based development of nitroxoline derivatives as potential multifunctional anti-Alzheimer agents. Bioorg. Med. Chem. 23, 4442–4452. https://doi.org/10.1016/j.bmc.2015.06.010.

Lee, S., Lee, H., Kim, K.W., 2020. Magnetic resonance imaging texture predicts progression to dementia due toAlzheimer diseaseearlier than hippocampal volume. J. Psychiatry Neurosci. 45, 7–14. https://doi.org/10.1503/jpn.180171.

Lemes, L.F.N., De Ramos, G.A., De Oliveira, A.S., Da Silva, F.M.R., DeCouto, G.C., DaBoni, M.S., Guimarães, M., Bartolini, M., Nogueira, P.C.N., Silveira, E.R., Brand, G.D., Romeiro, N.C., Castro, N.G., Soares, L.A.S., 2016. Cardanol-derived AChE inhibitors: towards the development of dual binding derivatives for Alzheimer's disease. Eur. J. Med. Chem. 108, 687–700. https://doi.org/10.1016/j.ejmech.2015.12.024.

Long, J.M., Holtzman, D.M., 2019. Alzheimer disease: an update on pathobiology and treatment strategies. Cell 179, 312–339. https://doi.org/10.1016/j.cell.2019.09.001.

Maalej, E., Chabchoub, F., Oset-Gasque, M.J., Esquivias-Pérez, M., González, M.P., Monjas, L., Pérez, C., De Los Ríos, C., Rodríguez-Franco, M.I., Iriepa, I., Moraleda, I., Chioua, M., Romero, A., Marco-Contelles, J., Samadi, A., 2012a. Synthesis, biological assessment, and molecular modeling of racemic 7-aryl-9,10,11,12-tetrahydro-7*H*-benzo[7,8]chromeno[2,3-*b*]quinolin-8-amines as potential drugs for the treatment of Alzheimer's disease. Eur. J. Med. Chem. 54, 750–763. https://doi.org/10.1016/j.ejmech.2012.06.038.

Mahdavi, M., Saeedi, M., Gholamnia, L., BehzadJeddi, S.A., Sabourian, R., Shafiee, A., Foroumadi, A., Akbarzadeh, T., 2017. Synthesis of novel tacrine analogs as acetylcholinesterase inhibitors. J. Heterocyclic Chem. 54, 384–390. https://doi.org/10.1002/jhet.2594.

Maalej, E., Chabchoub, F., Samadi, A., De los Ríos, C., Perona, A., Morreale, A., Marco-Contelles, J., 2011b. Synthesis, biological assessment and molecular modeling of 14-aryl-10,11,12,14-tetrahydro-9H-benzo[5,6] chromeno[2,3-b]quinolin-13-amines. Bioorg. Med. Chem. Lett. 21, 2384–2388. https://doi.org/10.1016/j.bmcl.2011.02.094.

Mahdavi, M., Hariri, R., Mirfazli, S.S., Lotfian, H., Rastergari, A., Firuzi, O., Edraki, N., Larijani, B., Akbarzadeh, T., Saeedi, M., 2019. Synthesis and biological activity of some benzochromenoquinolinones: tacrine analogs as potent anti-Alzheimer's agents. Chem. Biodivers. 16, e1800488.

Makhaeva, G.F., Kovaleva, N.V., Boltneva, N.P., Lushchekina, S.V., Astakhova, T.Y., Rudakova, E.V., Proshin, A.N., Serkov, I.V., Radchenko, E.V., Palyulin, V.A., Bachurin, S.O., Richardso, R.J., 2020a. New hybrids of 4-amino-2,3-polymethylene-quinoline and p-tolylsulfonamide as dual inhibitors of acetyl- and butyrylcholinesterase and potential multifunctional agents for Alzheimer's disease treatment. Molecules 25, 3915. https://doi.org/10.3390/molecules25173915.

Makhaeva, G.F., Kovaleva, N.V., Rudakova, E.V., Boltneva, N.P., Lushchekina, S.V., Faingold, I.I., Poletaeva, D.A., Soldatova, Y. V., Kotelnikova, R.A., Serkov, I.V., Ustinov, A.K., Proshin, A.N., Radchenko, E.V., Palyulin, V.A., Richardson, R.J., 2020b. New multifunctional agents based on conjugates of 4-amino-2,3-polymethylenequinoline and butylated hydroxytoluene for Alzheimer's disease treatment. Molecules 25, 5891. https://doi.org/10.3390/molecules25245891.

Mantoani, S.P., Chierrito, T.P.C., Vilela, A.F.L., Cardoso, C.L., Martínez, A., Carvalho, I., 2016. Novel triazole-quinoline derivatives as selective dual binding site acetylcholinesterase inhibitors. Molecules 21, 193. https://doi.org/10.3390/molecules21020193.

Marasco, D., Vicidomini, C., Krupa, P., Cioffi, F., Huy, P.D.Q., Li, M. S., Florio, D., Broersen, K., De Pandis, M.F., Roviello, G.N., 2021. Plantisoquinolinealkaloids as potential neurodrugs: A comparative study of the effects of benzo[*c*]phenanthridine and berberine-based compounds on β-amyloid aggregation. Chem. Biol. Interact. 334,. https://doi.org/10.1016/j.cbi.2020.109300 109300.

Marco, J.L., DelosRíos, C., Carreiras, M.C., Baños, J.E., Badí, A., Viva, N.M., 2001. Synthesis and acetylcholines-terase/butyrylcholinesterase inhibition activity of new tacrine-like analogues. Bioorg. Med. Chem. 9, 727–732. https://doi.org/10.1016/s0968-0896(00)00284-4.

Mo, J., Yang, H.Y., Chen, T.K., Li, Q.H., Lin, H.Z., Feng, F., Liu, W. Y., Qu, W., Guo, Q.L., Chi, H., Chen, Y., Sun, H.P., 2019. Design, synthesis, biological evaluation, and molecular modeling studies of quinoline-ferulic acid hybrids as cholinesterase inhibitors. Bioorg. Chem. 93. https://doi.org/10.1016/j.bioorg.2019.103310.

Munir, R., Ziaur-rehman, M., Murtaza, S., Zaib, S., Javid, N., Iftikhar, K., Athar, M.M., Khan, I., 2021. Microwave-assisted synthesis of (piperidin-1-yl)quinolin-3-yl) methylene)hydrazine-carbothioamides as potent Inhibitors of cholinesterases: a biochemical and in silico approach. Molecules 26, 656–687. https://doi.org/10.3390/molecules26030656.

Musiol, R., 2017. An overview of quinoline as a privileged scaffold in cancer drug discovery. Expert. Opin. Drug Discov. 12, 583–597. https://doi.org/10.1080/17460441.2017.1319357.

Nainwal, L.M., Tasneem, S., Akhtar, W., Verma, G., Khan, M.F., Parvez, S., Shaquiquzzaman, M., Akhter, M., Alam, M.M., 2019. Green recipes to quinoline: a review. Eur. J. Med. Chem. 164, 121–170. https://doi.org/10.1016/j.ejmech.2018.11.026.

Najafi, Z., Saeedi, M., Mahdavi, M., Sabourian, R., Khanavi, M., Tehrani, M.B., Moghadam, F.H., Edraki, N., Karimpor-Razkenari, E., Sharifzadeh, M., Foroumadi, A., Shafiee, A., Akbarzadeh, T., 2016. Design and synthesis of novel anti-Alzheimer's agents: acridine-chromenone and quinoline-chromenone hybrids. Bioorg. Chem. 67, 84–94. https://doi.org/10.1016/j.bioorg.2016.06.001.

Nqoro, X., Tobeka, N., Aderibigbe, B.A., 2017. Quinoline-based hybrid compounds with antimalarial activity. Molecules 22, 2268–2290. https://doi.org/10.3390/molecules22122268.

Nugraha, R.Y.B., Faratisha, I.F.D., Mardhiyyah, K., Ariel, D.G., Putri, F.F., Winarsih, N.S., 2020. Antimalarialproperties ofisoquinolinederivative fromStreptomyces hygroscopicus subsp.hygroscopicus: an in silico approach. Biomed. Res. Int., 6135696 https://doi.org/10.1155/2020/6135696.

Obulesu, M., Jhansilakshmi, M., 2014. Neuroinflammation in Alzheimer's disease: an understanding of physiology and pathology. Int. J. Neurosc. 124, 227–235. https://doi.org/10.3109/00207454.2013.831852.

Pan, Y.S., Wang, Y.L., Wang, Y.J., 2020. Investigation of causal effect of a trial fibrillation on Alzheimer dise-ase: A mendelian randomization study. J. Am. Heart Assoc. 9, e014889. https://doi.org/10.1161/JAHA.119.014889.

Patil, R., Chavan, J., Patel, S., Beldar, A., 2021. Advances in polymer based friedlander quinolinesynthesis. Turk. J. Chem. 45, 1299–1326. https://doi.org/10.3906/kim-2106-5.

Petruczynik, A., Tuzimski, T., Plech, T., Misiurek, J., Szalast, K., Szymczak, G., 2019. Comparison of anticancer activity and HPLC-DAD determination ofselectedisoquinoline alkaloids from Thalictrum foetidum, Ber-berissp. and Chelidonium majus extracts. Molecules 24, 3417. https://doi.org/10.3390/molecules24193417.

Pourabdi, L., Khoobi, M., Nadri, H., Moradi, A., Moghadam, F.H., Emami, S., Mojtahedi, M.M., Haririan, I., Forootanfar, H., Ameri, A., Foroumadi, A., Shafiee, A., 2016. Synthesis and structure-activity relationship study of tacrine-based pyrano[2,3-*c*]pyrazoles targeting AChE/BuChE and 15-LOX. Eur. J. Med. Chem. 123, 298–308. https://doi.org/10.1016/j.ejmech.2016.07.043.

Prati, F., Bergamini, C., Fato, R., Soukup, O., Korabecny, J., Andrisano, V., Bartolini, M., Bolognesi, M.L., 2016. Novel 8-hydroxyquinoline derivatives as multitarget compounds for the treatment of Alzheimer′s disease. ChemMedChem. 11, 1284–1295. https://doi.org/10.1002/cmdc.201600014.

Prince, M., Wimo, A., Guerchet, M., Ali, G.C., Wu, Y.T., Prina, M., 2015. World Alzheimer report. The global impact of dementia: ananalysis of prevalence, incidence, cost and trends. Alzheimer's disease international. pp. 1-80. https://www.alz.co.uk/research/WorldAlzheimerReport.

Przybyłowska, M., Dzierzbicka, K., Kowalski, S., Demkowicz, S., Daśko, M., Inkielewicz-Stepniak, I., 2022. Design, synthesis and biological evaluation of novel *N*-phosphorylated and *O*-phosphorylated tacrine derivatives as potential drugs against Alzheimer's disease. J. Enzyme Inhib. Med. Chem. 37, 1012–1022. https://doi.org/10.1080/14756366.2022.2045591.

Pudlo, M., Luzet, V., Ismaïli, L., Tomassoli, I., Iutzeler, A., Refouvelet, B., 2014. Quinolone-benzylpiperidine derivatives as novel acetylcholinesterase inhibitor and antioxidant hybrids for Alzheimer disease. Bioorganic. Med. Chem. 22, 2496–2507. https://doi.org/10.1016/j.bmc.2014.02.046.

Rani, S., Malik, A.K., Kaur, R., Kaur, R., 2016. A review for the analysis of antidepressant, antiepileptic and quinolone type drugs in pharmaceuticals and environmental samples. Crit. Rev. Anal. Chem. 46, 424–442. https://doi.org/10.1080/10408347.2016.1141670.

Rao, S.S., Raghunathan, R., Ekambaram, R., Raghunathan, M., 2009. In vitro activity of a new quinoline derivative, ER-2, against clinical isolates of Mycoplasma pneumoniae and Mycoplasma hominis. Antimicrob. Agents Chemother. 53, 5317–5318. https://doi.org/10.1128/AAC.00746-09.

Rivo, Y.B., Nugraha, Faratisha, I.F.D., Mardhiyyah, K., Ariel, D.G., Putri, F.F., Winarsih, N.S., Sardjono, T.W., Fitri, L.E., 2020. Antimalarial properties of isoquinolinederivative from Streptomyces hygrosco- picussub sp. hygroscopicus: an in silico approach. Biomed. ResInt 6135696. https://doi.org/10.1155/2020/6135696.

Rodríguez, Y.A., Gutiéerrez, M., Ramírez, D., Alzate-Morales, J., Bernal, C.C., Güiza, F.M., Romero Bohórquez, A.R., Romero Bohórquez, A.R., 2016. Novel *N*-allyl/propargyl tetrahydroquinolines: synthesis via Three-component cationic Imino Diels-Alder reaction, binding prediction, and evaluation as cholinesterase inhibitors. Chem. Bio.l Drug Des. 88, 498–510. https://doi.org/10.1111/cbdd.12773.

Rüb, U., Stratmann, K., Heinsen, H., Seidel, K., Bouzrou, M., Korf, H.W., 2017. Alzheimer's disease: characterization of the brain sites of the initial tau cytoskeletal pathology will improve the success of novel immunological anti-Tau treatment approaches. J. Alzheimer's Dis. 57, 683–696. https://doi.org/10.3233/JAD-161102.

Ryan, T.M., Roberts, B.R., McColl, G., Hare, D.J., Doble, P.A., Li, Q.X., Lind, M., Roberts, A.M., Mertens, H.D.T., Kirb, N., Pham, C.L.L., Hinds, M.G., Adlard, P.A., Barnham, K.J., Curtain, C.C., Masters, C.L., 2015. Stabilization of nontoxic Aβ-oligomers: Insights into the mechanism of action of hydroxyquinolines in alzheimer's disease. J. Neurosci. 35, 2871–2884. https://doi.org/10.1523/JNEUROSCI.2912-14.2015.

Safarizadeh, H., Garkani-Nejad, Z., 2019. Molecular docking, molecular dynamics simulations and QSAR studies on some of 2-arylethenylquinoline derivatives for inhibition of Alzheimer's amyloid-beta aggregation: Insight into mechanism of interactions and parameters for design of new inhibitors. J. Mol. Graph. Model. 87, 129–143. https://doi.org/10.1016/j.jmgm.2018.11.019.

Sang, Z., Pan, W., Wang, K., Ma, Q.G., Yu, L.T., Liu, W.M., 2017. Design, synthesis and biological evaluation of 3,4-dihydro-2(1*H*)-quinoline-*O*-alkyl-amine derivatives as new multipotent cholinesterase/ monoamine oxidase inhibitors for the treatment ofAlzheimer's disease. Bioorg. Med. Chem. 25, 3006–3017. https://doi.org/10.1016/j.bmc.2017.03.070.

Shachar, D.B., Kahana, N., Kampel, V., Warshawsky, A., Youdim, M.B.H., 2004. Neuroprotection by a novel brain permeable iron chelator, VK-28, against 6-hydroxydopamine lession in rats. Neuropharmacol. 46, 254–263. https://doi.org/10.1016/j.neuropharm.2003.09.005.

Shaik, J.B., Palaka, B.K., Penumala, M., Kotapati, K.V., Devineni, S. R., Eadlapalli, S., Darla, M.M., Ampasala, D.R., Vadde, R., Amooru, G.D., 2016. Synthesis, pharmacological assessment, molecular modeling and in silico studies of fused tricyclic coumarin derivatives as a new family of multifunctional anti-Alzheimer agents. Eur. J. Med. Chem. 107, 219–232. https://doi.org/10.1016/j.ejmech.2015.10.046.

Shang, X.F., Morris-Natschke, S.L., Liu, Y.Q., Guo, X., Xu, X.S., Goto, M., Li, J.C., Yang, G.Z., Le, K.H., 2018. Biologically activequinolineand quinazoline alkaloids part I. Med. Res. Rev. 38, 775–828. https://doi.org/10.1002/med.21466.

Sharma, A., Kumar, Y., 2009. Nature's derivative(s) as alternative anti-Alzheimer's disease treatments. J. Alzheimers Dis. Rep. 3, 279–297. https://doi.org/10.3233/ADR-190137.

Shen, T., Pu, J., Si, X., Ye, R., Zhang, B., 2016. An update on potential therapeutic strategies for Parkinson's disease based on pathogenic mechanisms. Expert Rev. Neurother. 16, 711–722. https://doi.org/10.1080/14737175.2016.1179112.

Silva, D., Chioua, M., Samadi, A., Agostinho, P., Garcão, P., Lajarín-Cuesta, R., de los Ríos, C., Iriepa, I., Moraleda, I., Gonzalez-Lafuente, L., Mendes, E., Pérez, C., Rodríguez-Franco, M.I., Marco-Contelles, J., Carmo Carreiras, M., 2013. Synthesis, pharmacological assessment, and molecular modeling of acetylcholinesterase/butyrylcholinesterase Inhibitors: effect against amyloid-β-Induced neurotoxicity. ACS Chem. Neurosci. 4, 547–565. https://doi.org/10.1021/cn300178k.

Solis Jr, E., Hascup, K.N., Hascup, E.R., 2020. Alzheimer's Disease: The link between Amyloid-β and neurovascular dysfunction. J. Alzheimers Dis. 76, 1179–1198. https://doi.org/10.3233/JAD-200473.

Umar, T., Shalini, S., Raza, M.K., Gusain, S., Kumar, J., Ahmed, W., Tiwari, M., Hoda, N., 2018. New amyloid beta-disaggregating agents: synthesis, pharmacological evaluation, crystal structure and molecular docking of *N*-(4-((7-chloroquinolin-4-yl)oxy)-3-ethoxybenzyl)amines. Med. Chem. Commun. 9, 1891–1904. https://doi.org/10.1039/c8md00312b.

Wang, L., Esteban, G., Ojima, M., Bautista-Aguilera, O.M., Inokuchi, T., Moraleda, I., Iriepa, I., Samadi, A., Youdim, M.B.H., Romero, A., Soriano, E., Herrero, R., Fernández Fernández, A.P., Murillo, R.M., Marco-Contelles, J., Unzeta, M., 2014a. Donepezil + propargylamine + 8-hydroxyquinoline hybrids as new multifunctional metal-chelators, ChE and MAO inhibitors for the potential treatment of Alzheimer's disease. Eur. J. Med. Chem. 80, 543–561. https://doi.org/10.1016/j.ejmech.2014.04.078.

Wang, X.Q., Xia, C.L., Chen, S.B., Tan, J.H., Ou, T.M., Huang, S.L., Li, D., Gu, L.Q., Huang, Z.S., 2015c. Design, synthesis, and biological evaluation of 2-arylethenylquinoline derivatives as multifunctional agents for the treatment of Alzheimer's disease. Eur. J. Med. Chem. 89, 349–361. https://doi.org/10.1016/j.ejmech.2014.10.018.

Wang, Z.R., Hu, J.H., Yang, X.P., Feng, X., Li, X.S., Huang, L., Chan, A.S.C., 2018b. Design, synthesis, and evaluation of orally bioavailable quinoline-indole derivatives as innovative multitarget-

directed ligands: promotion of cell proliferation in the adult murine hippocampus for the treatment of Alzheimer's disease. J. Med. Chem. 61, 1871–1894. https://doi.org/10.1021/acs.jmedchem.7b01417.

Wang, X.Q., Zhao, C.P., Zhong, L.C., Zhu, D.L., Mai, D.H., Liang, M.G., He, M.H., 2018d. Preparation of 4-flexible amino-2-arylethenyl-quinoline derivatives as multi-target agents for the treatment of Alzheimer's disease. Molecules 23, 3100–3120. https://doi.org/10.3390/molecules23123100.

Xia, C.L., Wang, N., Guo, Q.L., Liu, Z.Q., Wu, J.Q., Huang, S.L., Ou, T.M., Tan, J.H., Wang, H.G., Li, D., Huang, Z.S., 2017. Design, synthesis and evaluation of 2-arylethenyl-N-methylquinolinium derivatives as effective multifunctional agents for Alzheimer's disease treatment. Eur. J. Med. Chem. 130, 139–153. https://doi.org/10.1016/j.ejmech.2017.02.042.

Yang, X., Cai, P., Liu, Q., Wu, J., Yin, Y., Wang, X., Kong, L., 2018. Novel 8-hydroxyquinoline derivatives targeting β-amyloid aggregation, metal chelation and oxidative stress against Alzheimer's disease. Bioorganic. Med. Chem. 26, 3191–3201. https://doi.org/10.1016/j.bmc.2018.04.043.

Youdim, M.B.H., 2006. The path from anti Parkinson drug selegiline and rasagiline to multifunctional neuroprotective anti Alzheimer drugs ladostigil and m30. Curr. Alzheimer Res. 3, 541–550. https://doi.org/10.2174/156720506779025288.

Youdim, M.B.H., Fridkin, M., Zheng, H.L., 2004. Novel bifunctional drugs targeting monoamine oxidase inhibition and iron chelation as an approach to neuroprotection in Parkinson's disease and other neurodegenerative diseases. J. Neural. Transm. 111, 1455–1471. https://doi.org/10.1007/s00702-004-0143-x.

Youdim, M.B.H., Fridkin, M., Zheng, H.L., 2005. Bifunctional drug derivatives of MAO-B inhibitor rasagiline and iron chelator VK-28 as a more effective approach to treatment of brain ageing and ageing neurodegenerative diseases. Mech. Ageing Dev. 126, 317–326. https://doi.org/10.1016/j.mad.2004.08.023.

Zaib, S., Munir, R., Younas, M.T., Kausar, N., Ibrar, A., Aqsa, S., Shahid, N., Asif, T.T., Alsaab, H.O., Khan, I., 2021. Hybrid quinoline-thiosemicarbazone therapeutics as a new treatment opportunity for Alzheimer's disease-synthesis, in vitro cholinesterase inhibitory potential and computational modeling analysis. Molecules 26, 6573. https://doi.org/10.3390/molecules26216573.

Zhu, J., Yang, H.Y., Chen, Y., Lin, H.Z., Li, Q., Mo, J., Bian, Y.Y., Pei, Y.Q., Sun, H.P., 2018. Synthesis, pharmacology and molecular docking on multifunctional tacrine-ferulic acid hybrids as cholinesterase inhibitors against Alzheimer's disease. J. Enzyme Inhib. Med. Chem. 33, 496–506. https://doi.org/10.1080/14756366.2018.1430691.

Zhu, J., Wang, L.N., Cai, R., Geng, S.Q., Dong, Y.F., Liu, Y.M., 2019. Design, synthesis, evaluation and molecular modeling study of 4-N-phenylaminoquinolines for Alzheimer disease treatment. Bioorg. Med. Chem. Lett. 29, 1325–1329. https://doi.org/10.1016/j.bmcl.2019.03.050.